
Research Articles: Behavioral/Cognitive

Insensitivity of place cells to the value of spatial goals in a two-choice flexible navigation task

Éléonore Duvelle^{1,2,3,4}, Roddy M. Grieves⁴, Vincent Hok^{1,2}, Bruno Poucet^{1,2}, Angelo Arleo³, Kate Jeffery⁴ and Etienne Save^{1,2}

¹Aix Marseille Univ, CNRS, LNC, Laboratory of Cognitive Neuroscience, Marseille, France.

²Vision Institute, Aging in Vision and Action Lab, CNRS-INSERM, University Pierre and Marie Curie, Paris, France.

³Vision Institute, Aging in Vision and Action Lab, CNRS-INSERM, University Pierre and Marie Curie, Paris, France.

⁴Institute of Behavioural Neuroscience, Division of Psychology and Language Sciences, University College London, 26 Bedford Way, London WC1H 0AP

<https://doi.org/10.1523/JNEUROSCI.1578-18.2018>

Received: 22 June 2018

Revised: 19 December 2018

Accepted: 21 December 2018

Published: 29 January 2019

Author contributions: x.D., V.H., B.P., and E.S. designed research; x.D. performed research; x.D., R.M.G., and B.P. contributed unpublished reagents/analytic tools; x.D. and R.M.G. analyzed data; x.D. and E.S. wrote the first draft of the paper; x.D., K.J.J., and E.S. wrote the paper; R.M.G., V.H., B.P., A.A., and K.J.J. edited the paper.

Conflict of Interest: The authors declare no competing financial interests.

Support for this work was provided by the CNRS, Aix-Marseille University (for E.S., V.H., B.P.). Support for A.A. was from ANR -- Essilor SilverSight Chair. Funding for E.D. was from the "Délégation Générale pour l'Armement" and the "Fondation pour la Recherche Médicale (code FDT20130928415), as well as a Wellcome Trust, UK grant to K.J. We would also like to thank Francesca Sargolini for providing data extraction programs, Pierre-Yves Jacob, Luca Leonardo Bologna, Candie Cohen, Paul de St. Blanquat and Laureline Logiaco for their general help and guidance and Clémence Asselin, Laurène Save and Julie Gougot for their help with experiments.

Correspondence: Prof. K Jeffery, Institute of Behavioural Neuroscience, Division of Psychology and Language Sciences, University College London k.jeffery@ucl.ac.uk

Cite as: J. Neurosci 2019; 10.1523/JNEUROSCI.1578-18.2018

Alerts: Sign up at www.jneurosci.org/alerts to receive customized email alerts when the fully formatted version of this article is published.

Accepted manuscripts are peer-reviewed but have not been through the copyediting, formatting, or proofreading process.

Copyright © 2019 Duvelle et al.

This is an open-access article distributed under the terms of the Creative Commons Attribution 4.0 International license, which permits unrestricted use, distribution and reproduction in any medium provided that the original work is properly attributed.

21 Acknowledgements: Support for this work was provided by the CNRS, Aix-Marseille
22 University (for E.S., V.H., B.P.). Support for A.A .was from ANR – Essilor SilverSight Chair.
23 Funding for E.D. was from the “Délégation Générale pour l’Armement” and the “Fondation
24 pour la Recherche Médicale (code FDT20130928415), as well as a Wellcome Trust, UK
25 grant to K.J. We would also like to thank Francesca Sargolini for providing data extraction
26 programs, Pierre-Yves Jacob, Luca Leonardo Bologna, Candie Cohen, Paul de St. Blanquat
27 and Laureline Logiaco for their general help and guidance and Clémence Asselin, Laurène
28 Save and Julie Gougot for their help with experiments.

29 **Abstract**

30 Hippocampal place cells show position-specific activity, thought to reflect a self-localization
31 signal. Several reports also point to some form of goal encoding by place cells. We
32 investigated this by asking whether they also encode the value of spatial goals, which is a
33 crucial information for optimizing goal-directed navigation. We used a continuous place
34 navigation task in which male rats navigate to one of two (freely chosen) unmarked locations
35 and wait, triggering the release of reward which is then located and consumed elsewhere.
36 This allows sampling of place fields, and dissociates spatial goal from reward consumption.
37 The two goals varied in the amount of reward provided, allowing assessment of whether the
38 rats factored goal value into their navigational choice, and of possible neural correlates of
39 this value.

40 Rats successfully learned the task, indicating goal localization, and they preferred higher-
41 value goals, indicating processing of goal value. Replicating previous findings, there was
42 goal-related activity in the out-of-field firing of CA1 place cells, with a ramping-up of firing rate
43 during the waiting period, but no general over-representation of goals by place fields, an
44 observation that we extended to CA3 place cells. Importantly, place cells were not modulated
45 by goal value. This suggests that dorsal hippocampal place cells encode space
46 independently of its associated value, despite the effect of that value on spatial behavior. Our
47 findings are consistent with a model of place cells in which they provide a spontaneously
48 constructed value-free spatial representation, rather than encoding other navigationally
49 relevant, but non-spatial, information.

50 **Significance statement**

51 We investigated whether hippocampal place cells, which compute a self-localization signal,
52 also encode the relative value of places, which is essential information for optimal navigation.
53 When choosing between two spatial goals of different value, rats preferred the higher-value

54 goal. We saw out-of-field goal firing in place cells, replicating previous observations that the
55 cells are influenced by the goal, but their activity was not modulated by the value of these
56 goals. Our results suggest that place cells do not encode all of the navigationally relevant
57 aspects of a place, but instead form a value-free “map” that links to such aspects in other
58 parts of the brain.

59

60

61 **Introduction**

62 Goal-directed navigation mobilizes a large network of brain areas, central to which is the
63 hippocampus. In mammals, the dorsal hippocampal CA1 and CA3 regions contain place
64 cells, the firing of which is localized to “place fields” and encodes an animal's position in an
65 environment (O’Keefe and Dostrovsky, 1971; Moser et al., 2008). The dorsal hippocampus is
66 important for place navigation (Morris et al., 1982; Moser et al., 1995) and knowing whether
67 place cells encode information about spatial goals is fundamental to understanding
68 navigation mechanisms. The focus of the present study is whether the values of spatial goals
69 are encoded by the hippocampus.

70 Evidence that hippocampal neurons may encode goal locations differently from neutral
71 places is mixed (Poucet and Hok, 2017). Some studies have reported no goal
72 responsiveness (Speakman and O’Keefe, 1990; Jeffery et al., 2003; Zinyuk et al., 1999;
73 Grieves et al., 2016; Spiers et al., 2017) while others have found increased activity during
74 goal approach (Eichenbaum et al., 1987; Wiener, 1993, Breese et al., 1999). Recent studies
75 have observed an increased population firing, occurring away from the place field location, at
76 the goal (Hok et al., 2007a; Hok et al, 2007b; Hok et al, 2013; Hayashi et al., 2016). Finally,
77 other studies have shown that place fields migrate towards, or over-represent, goal locations
78 (Hollup et al., 2001; Kobayashi et al., 2003; Lee et al., 2006; Dupret et al., 2010, McKenzie et
79 al., 2013, Tryon et al., 2017). Collectively, these studies suggest that the occurrence of goal-
80 coding depends on a conjunction of factors such as task demands, inter-trial continuity, goal
81 novelty or trajectory stereotypy (repeated traversals of the same path).

82 Many navigational decisions require choosing the best among multiple goals, but few studies
83 have investigated the neural representation of goal value in the hippocampus. One such
84 study found no evidence of hippocampal encoding of goal value (Tabuchi et al., 2003), but
85 the spatial demands of the task were low. Others have suggested that place cells may
86 encode reward probability, action value, or reward expectation (Lee et al., 2012b, 2017;

87 Tryon et al., 2017) in linear mazes with no need for localizing a hidden goal. The amount of
88 reward available at a goal seems to affect some hippocampal phenomena such as local field
89 potential sharp-wave ripples (Singer and Frank, 2009) or patterns of sequential place cell
90 activation (“replay”; Ambrose et al., 2016), but these events happens at the time of reward
91 consumption and might reflect a reward-related feedback signal rather than a representation
92 of goal value. Thus, the question of whether place cells encode the value of spatial goals is
93 still open.

94 To address this question, we modified a task we have previously used to investigate
95 hippocampal goal coding (Hok et al., 2007a). The continuous navigation task (inspired from
96 Rossier et al., 2000) requires animals to navigate to an unmarked location in an open field
97 and wait there for a short duration (2s), after which an overhead dispenser releases a food
98 pellet which the animal has to search for. This task dissociates goal location from reward
99 consumption and allows recording of place fields, since the animal covers the whole
100 environment during its search for the reward. We previously found that CA1 place cells with
101 place fields located away from the goal fire spikes when the animal waits in the goal-zone
102 (Hok et al., 2007a), suggesting possible goal encoding. The task we designed has two
103 simultaneous goals that could provide different amounts of food, thus adding a value-based
104 decision-making component to this spatial task.

105 We found that rats were able to locate the two goals and preferentially navigate to the higher-
106 value goal, indicating behavioral sensitivity to this parameter. However, we did not observe
107 any place field overrepresentation of the goals, and saw no evidence of consistent goal value
108 coding by place cells. We conclude that place cells do not encode the value of spatial goals,
109 and that instead, this information must be combined with place information outside the
110 hippocampus.

111

112 **Materials and Methods**

113 *Subjects*

114 Six male Long–Evans rats (Janvier, St.-Berthevin, France) weighing 230–250 g and aged
115 around 2 months at the start of the experiment were used. Upon arrival, they were housed
116 two per cage in a colony room at $20 \pm 2^\circ\text{C}$, under a 12h/12h light-dark cycle beginning at
117 7 AM with free access to food and water. They were handled daily for 10 days. Before
118 behavioral training began, animals underwent a food deprivation procedure until they
119 reached 90% of free-feeding body weight and were maintained between 90-95 % of the free-
120 feeding weight during the study. After implantation surgery, they were housed individually.
121 The procedures were approved by the local ethics committee, authorization # A81212 and
122 the experiments were performed in accordance with European (2010/63/UE) and French
123 guidelines (Council Directive 87848 and permission # 13.24 to ES).

124 *Behavioral apparatus*

125 Training and electrophysiological recordings were performed in a 76 cm diameter circular
126 arena (Figure 1A) with 50 cm high black metallic walls and a grey-painted wooden floor. A
127 white cue covering 100° of arc was painted on the wall from top to bottom (making it 50 cm
128 high). The arena was located in the middle of a circular enclosure of opaque black curtains
129 2.5 cm diameter and 2.5 m high. A food dispenser (Med Associates, St Albans, VT, USA)
130 was located 2 m above the arena floor. When the dispenser was activated, one or more
131 (according to the experimental condition) 20 mg food pellets (A/P formula, Testdiet, St Louis,
132 MO, USA) dropped into the arena below. Pellets were released randomly through four
133 angled exit tubes and would roll to an unpredictable location in the arena (see Figure 1D for
134 example reward locations). As the animal had to forage over the entire arena to retrieve the
135 pellet(s), good sampling of all locations was obtained during recordings. Two cameras were
136 located above the arena, one allowing tracking of the animal's head position and the other

137 allowing visual detection of the pellet consumption (see details below). A radio set tuned to a
138 FM broadcast station and located above the apparatus was used to try to mask incidental
139 auditory cues. The apparatus was indirectly lighted by four symmetrically positioned LED
140 spots. The recording setup and computers for experimental control were located in an
141 adjacent room. The experimenter entered the recording room at the start and the end of a
142 sequence of sessions, and otherwise on rare instances to clean urine traces or disentangle
143 the recording cable.

144 -----
145 Insert Fig. 1 near here
146 -----

147 *Training procedure*

148 The rats were trained in an adapted version of the continuous navigation task used by Hok et
149 al. (2007a), hereafter called the two-goal navigation task. In Hok et al.'s study, the animals
150 were trained to locate a non-cued circular goal-zone and stay there for at least 2 s at which
151 time an overhead food dispenser was activated to release a 20 mg pellet. In the present
152 study, a similar procedure was used (Figure 1B) except that the animals could visit 2
153 symmetrically-placed non-cued goal-zones (20 cm diameter). Staying in either of the 2 goal-
154 zones for 2 s triggered the dispenser, after which the rat searched for and consumed the
155 pellet, at which point that trial terminated and the next began.

156 Training was performed in 4 steps. For each step, two consecutive 16-min training sessions
157 were conducted each day until the animals reached a learning criterion of 2 visits per goal-
158 zone and per minute. The rat was left in the arena between sessions and was returned to its
159 home cage at the end of the sequence. The arena floor was then wiped with water to reduce
160 and disperse local olfactory cues. The training steps were as follows:

- 161 (1) In step 1, a linoleum disc (20 cm of diameter) was placed on the floor, cueing one of
162 the two goal-zones during the first session. The dispenser was automatically
163 activated upon detection of the animal in the cued goal-zone. In the second session,
164 the disc was removed and the animal was rewarded when it entered the non-cued
165 goal-zone. On the following day, the same procedure was repeated for the other goal-
166 zone.
- 167 (2) In step 2, the animal had to stay in each goal-zone for a delay that gradually
168 increased across days in order to automatically activate the dispenser. The delay was
169 increased from 0.5 s to 2 s in 0.5 s steps every other day, over successive training
170 sessions using the same goal location. A similar sequence of daily sessions with
171 exposure to each goal-zone (marked followed by unmarked sessions) was conducted
172 as in step 1.
- 173 (3) In step 3, the two goal-zones were simultaneously available during a session. Each
174 day, a session with the marked goal-zones was followed by a session with the
175 unmarked goal-zones.
- 176 (4) Step 4 was the final form of this task, in which the two unmarked goal-zones were
177 simultaneously available during each of the 2 daily sessions. The reward was
178 released after a 2 s delay spent in a goal-zone. In order to obtain a similar number of
179 visits to each goal-zone during a session, a 5 s refractory period (minimum time
180 between two consecutive dispenser activations from the same goal zone) was used.
181 This meant that the rat had to spend more than 3 s outside of a goal zone before
182 being able to re-activate it. Successful visits to the goal-zones were consistently
183 followed by a foraging episode to retrieve the pellet. Once the pellet was found and
184 eaten, the animal returned immediately to a goal-zone. At the end of training, animals
185 that had a significant bias towards one of the goals were submitted to a training
186 session where that goal-zone was extinct, followed by a normal session, repeated
187 twice each day and this until they showed no significant preference for a specific goal.

188 The overall training phase lasted approximately 6 weeks. Only post-training behavioral
189 data were analyzed.

190 *Electrode implantation*

191 Following training, animals underwent surgery for electrode implantation above the right
192 dorsal hippocampus. Four rats were implanted above the CA1 field (aiming to collect CA1
193 followed by CA3 data) and – in order to eliminate possible experience-dependent effects on
194 results – 2 rats directly above the CA3 field (coordinates relative to Bregma, AP -3.8 mm, L -
195 3.0 mm, DV to dura -1.5 mm for CA1, -2.5 mm for CA3, Paxinos and Watson, 2007). A
196 drivable bundle of four tetrodes (Kubie, 1984) was implanted surgically under general
197 anesthesia using ketamine 60 mg/kg (Imalgène 1000, Merial, France; i.p.) and medetomidine
198 0.25 mg/kg (Domitor, Janssen, France; i.p.). Each tetrode was composed of four twisted 25-
199 μm nichrome wires. The four tetrodes formed a bundle threaded through a length of 30-
200 gauge stainless steel tubing. Each wire was connected to a pin of an 18-pin Mill-Max
201 connector. The tubing was attached to the central pin of the connector and served as the
202 animal ground as well as a guide for the tetrodes. The connector, tubing and 3 drive screws
203 were embedded in acrylic to form a triangle. The tetrodes could be lowered in the brain by
204 turning the 3 drive screws (1 turn \approx 450 μm) inserted in nylon cuffs cemented to the skull.
205 Before surgery, the wire tips were gold-plated to reduce their impedance to 200-400 k Ω
206 (measured at 1 kHz). Pre- and post-surgery treatments included a long-acting antibiotic
207 (amoxicillin, 150 mg/kg, s.c.) and an analgesic (buprenorphine, 0.05 mg/kg, s.c.). After
208 surgery, the animals were placed in a recovery room (22°C) for 3 days before being returned
209 to the colony room.

210 *Screening and recording*

211 Following a recovery period of at least 10 days post-surgery, rats were screened daily while
212 performing the 2-goal navigation task. If single-unit signals were considered of sufficient

213 amplitude, the recording protocol began. Otherwise, the electrodes were lowered by
214 approximately 28-56 μm and the rat was returned to its home cage. A delay of 24 hours was
215 interposed between successive screening sessions.

216 During screening and recording, a cable connected the recording system via a turning
217 commutator to the headstage (containing an operational amplifier, TLC 2272, Texas
218 Instruments) plugged into the rat's microdrive. A pulley and weight system helped to
219 compensate for the weight of the recording cable. Neural activity was recorded using 16-
220 channel Neuralynx hardware (Bozeman, MT, USA) controlled by a SciWorks acquisition
221 system (Datawave, Loveland, CO, USA). Local field potentials (LFPs) were sampled
222 continuously from one channel at a rate of 724 Hz (gain 1000, filtered 1 Hz - 475 Hz). Unit
223 signals were amplified 10,000 times and filtered (0.3 Hz - 6 kHz). During recording,
224 waveforms with amplitudes exceeding an experimenter-set threshold were sampled at 32
225 kHz and stored.

226 A single red light-emitting diode was connected at the back of the headstage, allowing
227 monitoring of the animal's head position with a 50Hz sampling rate by a tracking system
228 (Videotrack, Viewpoint, France). The tracking system was interfaced with the recording
229 software and the pellet delivery device so that detection of the LED in a goal-zone for 2s
230 automatically triggered an event-flag, together with appropriate activation of the reward
231 dispenser. The activation of the dispenser produced a small sound, as did the pellet(s)
232 landing on the arena floor. An additional event-flag was manually entered as a keypress, the
233 time-stamp of which was automatically saved by the recording system, when the animal was
234 seen to eat a pellet by an experimenter watching a screen. In addition to the Videotrack
235 system that was used to detect the animal in the goal-zones, a Datawave tracker (50Hz
236 sampling rate) was used to combine the animal's head position with unit signals.

237 The recording protocol included one of two types of sequences of four 16-min sessions each
238 (Figure 1C). On a given day, either a 1vs0 or a 1vs3 sequence was performed. The 1vs0

239 sequence consisted of alternating 1:1 sessions (each successful goal visit released 1 pellet)
240 with 1:0 sessions (one of the goals did not release a pellet). Sequences always started with a
241 1:1 session, and the choice of which goal set to 0 was reversed between the first and second
242 1:0 sessions. The 1vs3 sequence similarly alternated 1:1 and 1:3 sessions (where one of the
243 goals provided three pellets, released at 200 ms intervals). Similarly, the side of the goal
244 providing 3 pellets was swapped between the first and second 1:3 session. As in training, a
245 goal could not be re-activated during the 5s following its activation, to promote visits of the
246 two goals even in value-changing conditions. Figure 1D shows an example of goal activation
247 and pellet consumption behavior in a 1-3 sequence, spatially and temporally. Importantly, no
248 exterior signal indicated session change and the transition between sessions was
249 continuous; rats could only rely on the reward provided by each goal to estimate goal values.

250 At the end of the first day, the electrodes were left in place to leave the possibility to record
251 the same neurons in the other sequence on the next day. Once signals were recorded in
252 each sequence, tetrodes were moved of 0-1/8th of screw turn (~0-50 μ m).

253 *Data analysis – position-tracking and behavior*

254 All analyses and statistics were performed using the Python Programming Language, apart
255 from data conversion and Local Field Potential (LFP) analyses, implemented in MATLAB
256 (The MathWorks, Inc., Natick, Massachusetts, United States).

257 First, out of arena (mis-tracked) points were removed and positions were speed-filtered such
258 that any point with instantaneous speed > 150 cm/s was removed. Missing positions were
259 interpolated and all positions smoothed using a moving average over 9 points. Instantaneous
260 speed was computed on a window of 3 position data points, then smoothed with a moving
261 average over 9 positions points. Speed data were used to filter spuriously high speed tracked
262 positions (see above). Then, speed was re-computed on corrected position data and used to

263 compute speed-filtered occupancy and rate maps. An example of corrected position data for
264 a sequence of sessions is shown on Figure 1E.

265 Color-coded occupancy maps were built to visualize the distribution of the time spent by the
266 rat in various parts of the environment. Position data were binned into 32 x 32 bins (approx.
267 2.3 cm²) and dwell time in each bin computed to visualize the distribution of position of the rat
268 (see Figure 1E for examples). We also compared the occupancy in the goal locations to
269 symmetrical, control locations of the same size, offset by a 90 degree rotation. To quantify
270 possible biases in goal choice, we calculated a Spatial Preference (SP) Index as follows:

$$\text{Spatial Preference index} = \frac{(a - b)}{(a + b)}$$

271 where a = number of correct (longer than 2s) visits to the left goal zone and b = number of
272 correct visits to the right goal zone. Left/right referred to the position of each goal-zone with
273 respect to the cue-card. To quantify the preference for a goal depending on its value (i.e.
274 amount of reward provided), a Value Preference (VP) Index was computed using the same
275 method as spatial preference but where a represented the number of visits to the high value
276 goal zone and b the number to the low value goal zone. Spatial and Value preference indices
277 were computed either on whole sessions (16 min) to evaluate the global preference, or 1-min
278 bins to analyze the evolution of preference within sessions.

279 Speed profiles around task events (goal activation and reward consumption) were
280 constructed by computing the average speed profile time-locked on the event (4 seconds
281 before, 2 seconds after) for each session, then combining events of the same type (equal,
282 high or low value events) and averaging over sessions.

283 *Data analysis – single units*

284 **Spike-sorting** - Spike sorting was performed manually for each session so as to ensure
285 good quality isolation according to previously published methods (Hok et al., 2007) using the
13

286 Offline sorter software (Plexon, Dallas, TX, USA). Putative spiking events were grouped
287 based on waveform properties including waveform shape, peak amplitude, peak-to-valley
288 amplitude, spike amplitude at experimenter-defined times, and spike duration. Clusters with
289 more than 1% spikes with inter-spike intervals < 2 ms (indicating poor cluster discrimination)
290 were discarded (Alexander et al., 2016; Tanila et al., 2018).

291 **Rate maps** - Once putative cells had been separated, several types of firing rate maps were
292 built to visualize and analyze the spatial distribution of firing rate for each recording session.
293 First, each spike was associated to the closest (in time) recorded position. The recording
294 arena was divided, as mentioned above, into 32x32 square bins and rate maps were
295 computed as the number of spikes per bin divided by the time spent in each bin, using only
296 bins visited for more than 0.1s. Smoothed firing rate maps were built from these maps using
297 a Gaussian filter of sigma 0.7 (*scipy.ndimage.gaussian_filter* function). The same smoothing
298 parameters were applied to all types of rate maps used for the analysis. Speed-filtered firing
299 rate maps (whether smoothed or not) were constructed similarly but using speed-filtered
300 spikes and position (speed > 15 cm/s, Bendor and Wilson, 2012). Smoothed, speed-filtered
301 rate maps were used to detect place fields and compute spatial information content.
302 Smoothed 'low-speed' maps (speed <15 cm/s) were used to test for speed-dependent
303 alterations in firing. As will be shown later (in behavioral results), the mean speed of rats
304 during the goal activation delay is around 10 cm/s, which is why we chose the threshold of 15
305 cm/s to encompass most of the data at the goal within the low-speed condition but also data
306 with similar speed elsewhere in the arena. Finally, smoothed 'task-phase' maps were built
307 dissociating the reward-chasing phase (accumulation of episodes starting at a goal event
308 and ending at the pellet consumption event preceding the next goal activation) from the goal-
309 directed phase (starting from each pellet consumption event directly preceding a recorded
310 goal visit to the next goal-visit event, delay period included). Only the trials that included a
311 recorded food consumption event were used as some events were missed by the

312 experimenter (around $21\% \pm 10\%$ on average, computed using the difference between the
313 recorded and theoretical count).

314 Place fields were defined as a group of at least 9 contiguous pixels (sharing a side) with firing
315 rate exceeding 20% of the peak firing rate in the smoothed, speed-filtered (speed >15 cm/s)
316 rate map (Muller et al., 1987; Park et al., 2011; Brandon et al., 2014; Mamad et al., 2017;
317 Tanaka et al., 2018). Several parameters were computed on place fields: mean place field
318 firing rate, peak place field firing rate and place field size. Place fields and other cell
319 parameters were always defined for each session separately.

320 Information content (i.e. amount of information in bits per second conveyed about spatial
321 location by a cell; Skaggs et al., 1993) was calculated according to the formula:

$$\sum_i P_i \left(\frac{\lambda_i}{\lambda} \right) \log_2 \left(\frac{\lambda_i}{\lambda} \right)$$

322 where λ_i is the mean firing rate in each pixel, λ is the overall mean firing rate, and P_i is the
323 probability of the animal to be in the pixel i (i.e. dwelling time in pixel/total dwelling time).

324 This was computed over all pixels i of the smoothed speed-filtered (speed > 15 cm/s) rate
325 map.

326 A burst index was computed on whole-session data as the percentage of interspike intervals
327 shorter than one-fourth of each unit's mean interspike interval (Lee et al., 2012b). The
328 waveform duration was computed on each cluster's representative waveform (i.e. the
329 waveform of highest amplitude between all 4 channels, averaged over all spikes of a 1vs1
330 session) as the peak-to-trough duration.

331 All rate maps and spike plots presented here have been rotated to show the cue card at the
332 top of the figure, but analyses were performed on original, un-rotated data.

333 **Cell classification** - Using waveform and firing characteristics, each cluster (from a given
334 recording session) was automatically classified into a particular cell type. Place cells were
335 classified using the following criteria: burst index > 30%, waveform peak to trough duration >
336 300 μ s, mean speed-filtered firing rate between 0.05 and 7 Hz, at least 1 place field, and
337 spatial information content > 0.5 bits/second. A substantial amount of the other pyramidal
338 clusters had very low firing and no place field; these were estimated to be “silent cells”,
339 pyramidal neurons that have the ability to develop a place field under certain conditions
340 (Thompson and Best, 1989; Epsztein et al., 2011; Lee et al., 2012a; Diamantaki et al., 2018).
341 Only place cells were analyzed.

342 **Cell matching** - Once individual clusters were spike-sorted and classified, clusters belonging
343 to the same cell, recorded in different sessions, had to be identified. This was done in two
344 ways depending on the situation: *i*) for sessions recorded on the same day (i.e. without
345 unplugging the rat), clusters were manually associated to the same cell depending on their
346 position in the cluster space; *ii*) for sessions recorded on successive days, an automatized
347 procedure comparing the waveforms was used (Tolias et al., 2007, see below), followed by
348 manual refinement. For each tetrode, each cluster recorded on the first session of a given
349 day was compared to all clusters recorded during the first session of the next recording day,
350 when the electrodes had not been moved by more than \sim 0.5 screw turn (0-200 μ m). The
351 automated procedure was as follows: First, two distance measures (“Tolias distances”) were
352 computed on each pair of averaged waveforms (consisting of the average waveform for each
353 electrode of the tetrode). The first measure captures the difference in waveform shapes,
354 once scaled to the same amplitude, and the second describes the difference in amplitudes
355 across all 4 electrodes (for more details, see Tolias et al., 2007 and Powell and Redish,
356 2014). Then, a linear discriminant analysis method was applied that used the Tolias
357 distances to classify pairs of averaged waveforms as ‘same’ or ‘different’, as follows (Powell
358 and Redish, 2014). As a control group of pairs of ‘same’ waveforms, we used the distances
359 between the same units recorded from different sessions of the same day. As a control group

360 of 'different' waveforms, we used the distances between units recorded more than ~200 μm
361 apart. These two groups were fed to a linear discriminant analysis classifier
362 (*sklearn.discriminant_analysis.LinearDiscriminantAnalysis* Python function) which was then
363 used to categorize pairs of averaged waveforms into either the 'same' or 'different' group,
364 using the two Tolia distances as dimensions. Finally, the averaged waveforms from the two
365 clusters were manually checked by the experimenter using the result of the classifier as well
366 as the waveforms and the speed-filtered rate maps. The automated and manual method
367 agreed on more than 70% of all matched clusters (the cells belonging to the remaining <30%
368 pairs were considered to be different cells in the rest of the analysis). A similar proportion of
369 cluster pairs that were not matched by the algorithm (less than 30%) were matched by the
370 experimenter. This final classification was used for all the analyses. Unless stated otherwise,
371 when a given cell parameter was analyzed for a specific condition, the average of this
372 parameter over all instances of this cell in the condition was used.

373 **Goal over-representation by place fields** - To assess whether place fields over-represent
374 the goal locations, we computed a 'goal representation index' for each condition, indicating
375 the proportion of fields located at the goals. For cells recorded several times in the same
376 condition, the session with the highest mean firing rate was considered. Two methods were
377 employed and each was applied twice, once considering all fields and once considering only
378 one field per place cell (the largest). Both methods relied on defining 'goal fields' and 'control
379 fields'. For the first method, 'goal fields' were place fields with their center-of-mass (COM)
380 located inside any of the goals, and 'control' fields were those with a COM inside any of the
381 'control zones' – equivalent in size to the goals (see Figure 1E for an illustration of the
382 location of the control zones). For the second method, 'goal fields' were those closest to the
383 goals and 'control fields' were those closest to the control zones (thus, all fields were
384 included in method 2 but only a subset in method 1). For both methods, the 'goal
385 representation' index was equal to the number of 'goal fields' divided by the number of all
386 included fields (goal + control). A goal representation index of 50% would thus indicate

387 equivalent representation of the goals and the control zones. Finally, to assess whether the
388 ‘goal representation’ index was significantly higher than chance, we computed shuffled ‘goal
389 representation’ indices by randomly creating the same number of COMs as in the
390 corresponding data set, with their coordinates contained within the boundaries of the
391 recording arena, and re-computing the index from these; 1000 shuffled goal representation
392 indices were created for each condition. If the experimental value was above the 95th
393 percentile of the shuffled distribution it indicated over-representation of the goals (one-sided
394 test).

395 A different approach used was to assess whether the firing of place fields was different at the
396 goals than at the control zones. For this analysis, we compared the firing rate at goal zones
397 (defined spatially) of fields encroaching on a goal (i.e., if any of the pixels of the field was
398 contained in a goal zone) to the firing rate at control zones of fields encroaching on these
399 zones. Thus, different cells could contribute to each category and some cells might be used
400 both for the goal and control group - if they had a large enough field. The two groups of firing
401 rate were then compared using a Mann-Whitney U-test. To illustrate this analysis, cumulated
402 rate maps were computed by taking one z-scored, speed-filtered and smoothed rate map per
403 cell and per condition (in the case of multiple recordings of the cell, the rate map with highest
404 average firing rate was used) and averaging over all z-scored maps for each condition. Only
405 bins with data from at least 2 cells were included, and the final maps were smoothed again,
406 as described previously.

407 **Task phase correlates** - The place cell population might change its activity (or “remap”)
408 between the different sub-phases of the 2-goal navigation task (i.e. goal-directed phase vs
409 pellet-chasing phase), as suggested in Hok et al. (2007a), also see Markus et al. (1995). To
410 evaluate this, we built phase-filtered place cell maps (goal-directed vs reward-searching
411 phases, or slow vs high speed phases) and computed the Pearson’s R correlation coefficient
412 between the two types of maps for each cell. Then, we built a distribution of shuffled

413 correlations, i.e. between the same phase maps but from different cells recorded in the same
414 session (only including place cells). Thus, only sessions with at least two simultaneously
415 recorded place cells contributed to the shuffle distributions. Furthermore, to assess whether
416 the distribution of correlations obtained was bimodal, possibly indicating that different
417 subpopulations of place cell would behave differently, we used Hartigan's dip test (Hartigan
418 and Hartigan, 1985, Matlab implementation).

419 **Spatial firing stability-** To assess whether place cells were stable between successive
420 sessions, and whether reward-changing sessions would influence this, we computed the
421 Pearson's R correlation between smoothed, speed-filtered rate maps from one session to all
422 other sessions recorded for that cell (i.e. also across days).

423 **Overdispersion** - We computed the overdispersion of the place cell population or of
424 individual place cells in each condition. We used the same technique as Fenton et al. (2010),
425 to compute the population overdispersion, applied on smoothed rate maps (not speed-
426 filtered). We also computed the overdispersion of individual place cells similarly, only for cells
427 that contributed at least 20 passes through the place field (to be able to evaluate the
428 variance of the distribution of z values relatively accurately). Paired statistics were performed
429 comparing the average overdispersion per cell between conditions, either for all cells, or for
430 cells with a place field on the goal that changes value. Overdispersion was calculated as
431 follows (Fenton et al., 2010): the entire session was divided into 5s episodes and then an
432 expected number of spikes was computed per episode, using the following formula:

$$\mathbf{exp} = \sum_i r_i t_i$$

433 where r_i is the firing rate at location i and t_i is the time spent in location i during this pass.

434 Only passes with at least 5 expected action potentials ($\mathbf{exp} \geq 5$, equivalent to 1Hz) were

435 considered for the analysis as these would reflect passes through the place field. For each

436 pass, the normalized standard deviation of the expected number of spikes, z , was computed
 437 as follows:

$$z = \frac{(\text{obs} - \text{exp})}{\sqrt{\text{exp}}}$$

438 with obs representing the observed number of spikes during the pass. Finally, the
 439 overdispersion value was computed as the variance of the distribution of z values for all
 440 passes. As mentioned above, overdispersion was computed either for the whole place cell
 441 population (all passes combined together for a given session type, each cell contributing
 442 once per session type using the instance with the higher mean firing rate) or per cell
 443 (similarly, only one instance of each cell per session type was used).

444 **Analyses of goal activity** - Similar to behavior-related analysis, we first compared the firing
 445 rate at the goal zones (defined spatially) to the firing rate at control goal zones, for low or
 446 high speeds. We also calculated a Spatial Firing Preference index, defined temporally, to
 447 evaluate a spatial bias of goal firing as follows:

$$\text{Spatial firing preference} = \frac{(F_a - F_b)}{(F_a + F_b)}$$

448 where F_a = firing rate during left goal visits and F_b = firing rate during right goal visits. To
 449 address the question of value-coding at the population level, we first compared the firing rate
 450 at the high value goal zone to that of the low value goal zone. We also calculated a Value
 451 Firing Preference index for 1vs0 and 1vs3 sessions, to evaluate goal firing as a function of
 452 the expected reward magnitude. This was calculated in the same way as the **Spatial Firing**
 453 **Preference index** where F_a = firing rate during trials at the high value goal-zone and F_b =
 454 firing rate during trials at the low value goal-zone.

455 **Value coding** - To assess value-coding at the single cell level, we computed a similar value
 456 firing preference index, but between sessions and for each goal; in that case, F_a was the

457 firing at the goal when it was modified (value = 0 or 3) while F_b was the firing at the same
458 goal in the previous session (value = 1). This measured the relative amount of change in
459 firing following the change in goal value. To assess if this change was significant, we
460 computed a shuffle distribution, for the same cell and goal, of value firing preference indices
461 where the trials of the two conditions were shuffled. Only sessions with at least 5 visits to the
462 goal were used and 5000 shuffle values were computed. The data were then compared to
463 the shuffle distribution and deemed significantly higher than chance if they were higher than
464 the 97.5th percentile, or lower than chance if they were lower than the 2.5th percentile of the
465 distribution (two-sided test). A given cell was termed ‘transiently value-modulated’ if, at least
466 once, it significantly increased or decreased its firing in the value session, for at least one
467 goal. To assess actual value-encoding of cells, and not simple modulation by value, we
468 considered whether cells were consistently encoding value: a cell was termed ‘consistently
469 value coding’ if it was significantly changing its firing when value changed, for the majority of
470 sessions of the same type (and at least 2), and in the same direction (i.e. either increase or
471 decrease of firing).

472 **Peri-event time histograms (PETH)** – To assess whether activity at the goal had a specific
473 temporal profile during the delay period, PETHs time-locked to goal activation were
474 computed. Spike times for all trials in a session, i.e. 2 s visits to the goal-zone, were aligned
475 with the feeder activation event flag and accumulated in 100 ms bins to produce a PETH
476 covering 4 s before feeder activation to 2 s after activation. Then, each PETH was
477 normalized by its maximum so that we could average PETHs from different cells. When the
478 PETHs for different goals were combined (e.g., left and right), trials belonging to one or the
479 other goal were combined for each cell and then averaged to form the PETH of that cell.
480 When comparing the normalized firing rate during the delay, we used a bin of 1s instead of
481 0.1s. For the time order analysis, the individual normalized PETHs from each cell were
482 smoothed with a Gaussian filter of sigma = 150 ms.

483 *Data analysis – local field potentials*

484 Before analysis, all LFP data were removed of their direct current offsets, slowly changing
485 components, and running line noise using the Chronux toolbox (Bokil et al., 2010) *locdetrend*
486 function which subtracts the linear regression line fit within a 1s moving window and the
487 *rmlinesc* function which removes significant sine waves based on their F-statistic. Data were
488 also notch-filtered using a second-order digital filter at frequencies of 50, 150 and 250 Hz
489 (MATLAB function *iirnotch*, Q-factor 100). They were then resampled at 750 Hz using a
490 polyphase anti-aliasing filter (MATLAB function *resample*, pchip interpolation).

491 Time-frequency spectrograms were generated using the MATLAB function *spectrogram*,
492 these were comprised of 200 ms time windows with a 50% overlap. Analyses focused on the
493 theta frequency band (4-12 Hz). Running power for each frequency band was calculated as
494 the mean power in that band, frequency was calculated as the frequency associated with the
495 maximum power. We then extracted these values during each goal activation event (4s
496 before, - 2s after) and aligned these windows to the event time point. These event-related
497 spectral perturbations (ERSPs) were then averaged within each session and normalized by
498 their mean and standard deviation (i.e. z-scored) with respect to random baseline events
499 (Ahmed and Mehta, 2012; Donnelly et al., 2014; Nishida et al., 2014) so that consistent
500 changes in spectral power or frequency across sessions could be assessed. We performed
501 the same tests on data composed of session averaged ERSPs and rat-averaged ERSPs for
502 all sessions.

503 We similarly calculated the power spectral density estimate (PSD) of the LFP data, using the
504 MATLAB *periodogram* function. This was computed for 500 logarithmically spaced points
505 between 0-300 Hz using a hamming window after data were zero-padded to the next highest
506 power of 2. This method was applied to the LFP truncated to include only the 4s before and
507 2s after each goal event. For each of these PSDs we calculated the maximum power
508 exhibited in the theta band and the frequencies associated with these maxima. We

509 performed the same tests on data composed of session-averaged PSDs and rat-averaged
510 PSDs for entire sessions (only session-averaged data are shown).

511 Statistical tests were conducted on the mean value per session within the time window, i.e.
512 low vs high (1vs0) theta power is the mean z-scored theta power (n sessions long) in the low
513 value goal zone compared to the mean z-scored theta power in the high value goal zone
514 (also n sessions long).

515 *Experimental Design and Statistical Analysis*

516 Unless stated otherwise, when all the data for a test were normally distributed (tested via
517 *scipy.stats.normaltest* that uses skew and kurtosis) we ran parametric tests such as t-tests,
518 while non-parametric tests (e.g. Mann-Whitney test for non-paired data, Wilcoxon signed-
519 rank test for paired data) were used otherwise. The Wilcoxon signed-ranked test was also
520 used to assess whether distributions of preference indices significantly differed from a
521 distribution of 0 mean – it assesses whether the distribution of values is symmetrically
522 distributed around 0. Boxplots were generally used to show data distribution, with the median
523 as a black horizontal line, the first (Q1) and third (Q3) quartiles as the box limits, $Q1 - 1.5 \times$
524 interquartile range (IQR, $Q3 - Q1$) as the bottom whisker and $Q3 + 1.5 \times$ (IQR) as the top
525 whisker. Distributions such as PETHs were compared to each other using the Kolmogorov-
526 Smirnov test. To assess the level of correlation between two samples, we computed
527 Pearson's R correlation coefficient (for example to test for remapping or for temporal order of
528 cell firing). To compare proportions, we performed binomial tests.

529 *Histology*

530 At the end of the study, rats were given a lethal dose of pentobarbital (Dolethal, Vetoquinol,
531 France; 100 mg/kg, 1 ml i.p.). The final position of the electrodes was marked by passing
532 anodal current through one of the wires of each tetrode (15 μ A for 30 s). Under deep
533 anesthesia, the rats were perfused transcardially, first with a saline solution (NaCl 9‰), then

534 with a formalin solution (4%). Their brains were extracted and left in a 30% glucose solution
535 for one or two days. Then, they were frozen with dry ice (carbon dioxide) and stored at -
536 80°C. The frozen brains were cut at 30 μ m intervals and stained with Cresyl Violet. They
537 were examined under a light microscope to determine the cannula track and the final position
538 of the electrodes. This information was combined with the distribution of neurons recorded
539 per electrode depth to determine the putative limits of CA1 and CA3 hippocampal fields.
540 Each unit was then associated to a putative hippocampal field (Figure 3 shows the estimated
541 trajectory of tetrodes for each rat).

542 **Results**

543 In the description that follows, we use the notation 1:0, 0:1 or 1:3, 3:1 to differentiate goal
544 value on left vs. right, respectively, and 1vs0 or 1vs3 if the specific goal location is not
545 relevant.

546 *Behavior – Rats' choices reflect goal value*

547 Six implanted rats performed a total of 224 sequences of 4 sessions. Only the sequences
548 providing exploitable neuronal signals were used for analysis (n = 117). Behavioral results
549 are similar if all sessions, even those without exploitable units, are included (data not shown).
550 The median number of 1vs0 sequences (1:0 or 0:1 sessions, interspersed with 1:1 sessions)
551 per rat was 8.5 (max = 21, min = 5) and the median number of 1vs3 sequences (1:3 or 3:1
552 sessions, interspersed with 1:1 sessions) was 8 (max = 19, min = 4). Unless stated
553 otherwise, the two 1:1 sessions were usually combined into 1vs1, and value-changing
554 sessions 1:0 and 0:1 (1:3 or 3:1) into 1vs0 (or 1vs3, respectively). The 1:1 sessions in the
555 middle of a sequence were not used as they could incorporate uncontrolled effects from the
556 previous session.

557 An example of goal choice behavior from a 1vs0 sequence of 4 sessions is shown in
558 Figure 1D, with the corresponding location of goal events (successful goal visits, at least 2
24

559 seconds spent in a goal location) and reward consumption. The goal visit rate, i.e. number of
560 goal events per minute, was 4.5 ± 0.15 (s.e.m across rats) in the 1vs1 condition, which is
561 higher than previous studies (e.g., mean goal visit rate was 2.1 successful goal visits / min in
562 Hok et al. (2007a). The average goal visit rate was 4.6 ± 0.1 visits / min in 1vs0 sessions and
563 3.7 ± 0.2 visits / min in 1vs3 sessions.

564 We then analyzed behavior both spatially and temporally. Spatially, we evaluated whether
565 goal locations were more visited than two control non-goal zones symmetrically positioned
566 and of the same size. To visualize this, we plotted the cumulated occupancy maps for each
567 of the conditions (Figure 2A), averaged over sessions, then rats. All maps clearly show a
568 high occupancy of the two goal locations in all conditions (including for the non-rewarded
569 goal in 1vs0 sessions), and a preference for the goal of high value in value-changing
570 sessions. Next, we compared the occupancy at the two goals (combined) to occupancy at
571 the control zones (combined), for each condition (see Figure 2B): occupancy at the goals
572 was always significantly higher than at the non-goal zones (1vs1: Wilcoxon, $W = 0$, $p = .02$;
573 1vs0: Wilcoxon, $W = -11.4$, $p = 9.1 \times 10^{-5}$; 1vs3: Wilcoxon, $W = -10.7$, $p = .0001$). In the 1vs1
574 condition, the occupancy for left and right goal was not different (Wilcoxon, $W = 0$, $p = .75$),
575 showing an absence of spatial bias, while comparing the high-value goal to low-value goal in
576 the 1vs0 condition yielded a significant difference ($W = 0$, $p = .027$). This was also the case
577 in the 1vs3 condition with a higher occupancy for the high-value goal compared to the low-
578 value goal (Wilcoxon, $W = 1.0$, $p = .046$). This preference developed steadily across the
579 course of a trial as shown by the behavioral value preference (VP) index computed per 1-min
580 bins (Figure 2C). The preference index should be around 0 if there is no preference and
581 towards 1 for a preference for the high-value goal. For 1vs1, the side preference is shown
582 instead and a value of 1 would indicate a preference for the left goal. The time course of
583 preference for the 1vs0 and 1vs3 conditions was compared to that of the side preference in
584 the 1vs1 and was found to be significantly different (1vs0 vs 1vs1, Kolmogorov-Smirnov $D =$
585 0.94 , $p = 3.1 \times 10^{-7}$; 1vs3 vs 1vs1, Kolmogorov-Smirnov $D = 0.88$, $p = 2.32 \times 10^{-6}$) while there

586 was no significant difference between the profile of value preference for 1vs0 and 1vs3
587 conditions (Kolmogorov-Smirnov $D = 0.38$, $p = .16$). Thus, rats' goal choice behavior was
588 controlled by the number of pellets obtained and not by the spatial location of the goal-zones.
589 Overall, rats demonstrated learning of the spatial and value aspects of the task.

590 -----
591 Insert Fig. 2 near here
592 -----

593 Temporally, we generated running speed profiles centered on the goal activation or the
594 reward consumption event, see Figure 2D. For reward consumption events, the average
595 speed as well as its standard deviation appear to drop just before the event, indicating a
596 relatively precise timing of the event. For goal events, velocity peaked just before goal zone
597 entry (i.e., around 2s before pellet release) and then dropped steeply, indicating that the rats
598 knew they were in the right zone. The average velocity during the goal period was not
599 different for left or right goals in 1vs1 condition (left goal: 10.4 ± 1 cm/s, right goal: 10.2 ± 1.6
600 cm/s, $t(5) = 0.57$, $p = .59$, paired t-test) or high-versus low-value goals (1vs0 condition, low-
601 value: 10.1 ± 1.6 cm/s, high-value: 9.9 ± 1.4 cm/s, $t(5) = 0.27$, $p = .79$; 1vs3 condition, low-
602 value: 9.6 ± 1 cm/s, high-value: 9.8 ± 0.8 cm/s, $t(5) = -1.1$, $p = .33$). Interestingly, even for
603 trials in the 1vs0 condition when no pellet was released and no sound was emitted by the
604 dispenser activation, the rats' speed increased again at the end of 2s (Figure 2D, middle –
605 right inset), indicating processing of time as well as space (similar results were reported in
606 Hok et al. 2007b, where the unique goal did not provide reward for 4 minutes).

607 To summarize, goal location, goal value and temporal duration all influenced the animals'
608 behavior in this task. Rats waited at the unmarked goal zones, indicating successful goal
609 location processing, they also showed a strong preference for the higher value goal,
610 indicating goal value processing, and they increased their running speed to exit the goal

611 zone even when the goal was unrewarded, indicating an uncued awareness of temporal
612 duration. Thus, rats clearly processed the spatiotemporal and value components of the task.

613 *Electrophysiology – single units*

614 We next looked at the activity of single pyramidal units, to see whether there was (a)
615 evidence of goal encoding of the types seen previously, and (b) evidence or not of goal value
616 processing. Previous reports have observed a form of goal coding either from the place fields
617 of CA1 place cells (Dupret et al., 2010) or from their out-of-field activity (Hok et al., 2007a).
618 To investigate this, we first asked whether place field or out-of-field activity encoded goal
619 locations in 1vs1 sessions. Next, we analyzed this activity for putative value encoding using
620 the value-changing sessions 1vs0 and 1vs3. Because of the well-established relationship of
621 place cell activity to locomotor behavior (McNaughton et al., 1983), we analyzed activity both
622 when the rat was actively engaged in goal processing (paused waiting at the goal, running
623 towards the goal, possibly planning a trajectory, etc.) vs incidentally traversing the region
624 during the reward-search phase.

625 A total of 157 unique putative pyramidal cells were recorded from the dorsal hippocampus of
626 6 rats performing the two-goal navigation task. Of these, 104 (66%, median = 10/rat, min = 3,
627 max = 41) were categorized as place cells, of which 59 cells were considered to be from the
628 CA1 hippocampal field (from 4 rats) and 45 cells from CA3 (from 5 rats). A summary of the
629 histology results is shown in Figure 3 and example CA1 and CA3 place cells are shown in
630 Figure 4.

631 -----
632 Insert Fig. 3 near here
633 -----

634 The number of unique place cells that could be matched for several days are as follows: 2
635 days: 61, 3 days: 33, 4 days: 23, 5 days: 8, 6 days: 7, 7 days: 3 (see methods for the Tolias

636 distance cross-day matching technique, relying on waveform similarities, and Figure 4B and
637 D for examples of cells recorded across 4 days). We also recorded 40 putative “silent cells”
638 (Thompson and Best, 1989) that had scarce firing and no detected place fields (24% of
639 pyramidal cells, median = 4/rat, min = 1, max = 22; 25 from CA1, 15 from CA3). Since their
640 firing was very low by definition (median speed-filtered firing = 0.06 Hz), we did not include
641 them in the present analysis but report that most of their firing was concentrated at the goal
642 locations.

643

644

Insert Fig. 34 near here

645

646 *General CA1 and CA3 differences*

647 First, we compared the general properties of CA1 and CA3 place cells (see Figure 4A and C
648 for examples of each). CA1 cells had a shorter waveform width (median = 500 μ s) compared
649 to CA3 cells (median = 531 μ s, Mann–Whitney $U = 920$, $p = .0068$) and the average firing
650 rate of CA1 place cells (median = 0.5 Hz) was lower than that of CA3 place cells (median =
651 1.1 Hz, Mann–Whitney $U = 815$, $p = .0008$). The 104 recorded place cells had 134 place
652 fields and the mean number of place fields per cell was not significantly different between
653 CA1 and CA3 (1.4 for CA1 cells, 1.7 for CA3 cells, Mann–Whitney $U = 1920$, $p = .12$).
654 However, CA3 place fields had a higher mean firing rate and peak firing rate compared to
655 CA1 fields (median firing of 73 CA1 place fields = 4.1 Hz, median firing of 61 CA3 place fields
656 = 5.7 Hz, Mann–Whitney $U = 1781$, $p = .046$; median of all CA1 peak place field firing = 9.2
657 Hz, median of all CA3 peak place field firing = 12.6 Hz, Mann–Whitney $U = 1726$, $p = .025$).
658 CA3 fields were also generally larger than CA1 ones (median size of CA1 place fields = 35
659 pixels, median size of all CA3 place fields = 75 pixels, Mann–Whitney $U = 1505.5$, $p = .0013$).

660 *Place fields do not over-represent goal locations*

661 To assess whether place cells would specifically represent the goal locations with their place
662 fields, we first analyzed place-specific firing when the rats were moving across the arena
663 (speed >15 cm/s), focusing on the 1vs1 condition. The 134 place fields were distributed
664 across the entire arena (Figure 5A shows the centers of mass, or COMs, of all place fields).
665 We analyzed either all place fields or only the largest place field per cell ($n = 101$). First, we
666 computed a 'goal representation' percentage using the number of COMs in the goals and
667 those located in equivalent control zones (see Methods). Place fields did not over-represent
668 the goal zones (when only place fields in the goal or control zones were considered, 64.7%
669 of 34 COMs were closer to the goals, n.s. compared to shuffled distribution; when all place
670 fields in the arena were considered, 56% of 134 COMs were closer to the goals, n.s.
671 compared to shuffle distribution). A similar absence of goal over-representation was found if
672 only the biggest place field for each place cell was taken into account (goal representation
673 percentage of 67% out of 27 place fields in a goal or control zone, n.s. compared to shuffled
674 distribution; goal representation percentage of 56% out of 104 place fields in the arena, n.s.
675 compared to shuffle distribution), or if the CA1 and CA3 populations were tested separately.
676 Similarly, comparing the number of cells that have a place field encroaching on either of the
677 goals ($n = 78$) to that of cells with a place field on any of the control non-goal zones ($n = 66$)
678 did not yield a significant difference (binomial test, $p = .35$). We also used an analysis
679 adapted from Dupret et al. (2010) which did not yield any over-representation of goals either
680 (data not shown). Finally, we noticed that CA1 place fields seemed more peripheral than
681 CA3 ones and compared the distance to the center of the arena of CA1 and CA3 COMs. We
682 found that CA3 fields were indeed more central, either when all place fields were used (mean
683 distance to arena center: 27.2 ± 7.2 cm for 73 CA1 place fields, 22.5 ± 8 cm for 61 CA3 place
684 fields, Mann–Whitney $U = 1393.0$, $p = .0002$) or when only the biggest place fields (1 per
685 place cell) were used (mean distance to arena center: 29.2 ± 7 cm for 59 CA1 place fields,
686 23.2 ± 7.8 cm for 45 CA3 place fields, Mann–Whitney $U = 783.0$, $p = .0004$). As this

687 difference was probably due to the difference in place field size between the two populations
688 (larger place fields should have a more central COM), we did not analyze it any further.

689 To conclude, place fields do not over-represent the spatial goals in this task, coherently with
690 previous findings in the single goal version of the task (Hok et al., 2007a) and in contrast with
691 other findings (Hollup et al., 2001; Dupret et al., 2010; Lee et al., 2012b) in which the over-
692 represented location was also a rewarded location.

693

694

Insert Fig. 5 near here

695

696 Place cells might not signal goal locations through the presence or absence of a place field,
697 but via modulations of firing rate. Thus, we compared the firing rate between goal and non-
698 goal zones, when place fields were detected to overlap on the zone of interest and, first,
699 when the rat was running (speed >15 cm/s). For illustration purposes, we averaged the
700 speed-filtered rate maps of all recorded place cells (normalized by z-scoring first) and no
701 goal over-representation was visible (Figure 5B). Regarding firing rates, as there was no
702 difference between the mean firing at the two goals (Mann–Whitney $U = 983.0$, $p = .23$), they
703 were combined, and this was the same for the two non-goals (Mann–Whitney $U = 649.0$, $p =$
704 $.562$). No difference in firing rate was observed between goals (median = 1.36 Hz, $n=78$) and
705 non-goals (median = 1.12 Hz, $n = 66$, Mann–Whitney $U = 2432.5$, $p = .57$). The same
706 analysis was applied on low-speed data (so, when the rat was waiting at the goal zone or
707 elsewhere) and did not evidence any difference either in firing rate, as far as place fields
708 were concerned (median firing at goals: 1.15 Hz, non-goals: 1.35 Hz, Mann–Whitney $U =$
709 2492.0 , $p = .743$, Figure 5C).

710 Finally, we considered whether place fields might remap depending on task conditions, i.e.
711 when the rat was waiting (speed < 15 cm/s) versus moving (speed > 15 cm/s), or when the
712 rat was searching for reward compared to when it was approaching the goal and waiting at
30

713 the goal ('goal-directed' phase, see methods). For this, we computed Pearson's correlation
714 coefficients for each place cell between 1) its rate map at low-speeds vs high-speeds, cf.
715 Figure 5D, or 2) its rate map during foraging vs goal-directed phases, see Figure 5E. A
716 shuffled distribution of correlations was computed in each case to estimate the distribution of
717 a randomly remapping population, by computing correlations between different cells
718 recorded during the same session (see Methods). In both cases, the shuffled distributions
719 were different from the data, the latter showing higher correlations (for the speed-related
720 correlations: Kolmogorov-Smirnov $D = 0.88$, $p = 9.5 \times 10^{-62}$, median of shuffle = -0.04, 95th
721 percentile of shuffle distribution = 0.32, median of data = 0.67; for the foraging vs goal-
722 directed correlations: Kolmogorov-Smirnov $D = 0.81$, $p = 1.6 \times 10^{-52}$, median of shuffle = -
723 0.04, 95th percentile of shuffle distribution = 0.29, median of data = 0.5). We also tested
724 whether the distribution of correlations were different from unimodality, as a bimodal
725 distribution of correlations could indicate that different subpopulations of place cells behaved
726 differently, i.e., partial remapping. For this, we used Hartigan's dip test (Hartigan and
727 Hartigan, 1985) and found that none of the two distributions of correlations were significantly
728 different from a unimodal distribution (correlations between different speed phases, dip
729 statistic = 0.028, $p = .817$; correlations between different task phases, dip statistic = 0.028, p
730 = .884). Finally, we individually looked at the maps with low (<0.2) correlation values to
731 assess whether this was due to individual cell remapping. In around 50% of the cases, the
732 place field location was not sampled enough in one of the conditions, spuriously creating a
733 low correlation. In around 45% of these low correlations cases, the maps had relatively low
734 firing and the correlations values could probably not be very accurately computed. In 9% of
735 cases and only for goal-directed vs reward search comparisons, we found that the place field
736 disappeared in one of the conditions, but this represented only 3 cells (0 in the speed-based
737 correlations) and we do not believe this to be of any significance. Thus, the place cell
738 population did not globally remap between the different behavioral phases. At first glance,
739 this seems to contrast with several studies that previously found task-based remapping
740 (Wiener et al., 1989; Markus et al., 1995; Siegel et al., 2008; Ainge et al., 2012). However,
31

741 the task phases compared in these studies were always performed in blocks. In tasks that
742 alternate two types of behavior, like the present study, no remapping is found (Trullier et al.,
743 1999; Zinyuk et al., 2000; Siegel et al., 2008).

744 Overall, our results so far indicate that the two spatial goals are not over-represented by
745 place fields and that the population activity is encoding space in a homogeneous manner
746 regardless of the moment-to-moment behavior or putative intention of the rat.

747 *Is there out-of-field spatial goal coding?*

748 As established in previous studies (Hok et al., 2007a, 2007b, 2013), place cells express
749 'goal-related' activity, increased out-of-field firing at the goal, in a single goal version of the
750 continuous navigation task. This signal is sparse at the single-cell level but clear at the
751 population level. Thus, we asked whether goal-related firing was present in our task by
752 analyzing out-of-field activity at the goal, whether in its firing rate, or its temporal aspect.
753 First, we analyzed the out-of-field firing rate of place cells at goal locations (i.e. when no
754 detected place field, whether primary, secondary or other, was encroaching on the goals),
755 compared to similar out-of-field firing but at the control zones. At low speeds, the firing at the
756 goal was significantly higher than in the corresponding non-goal zone (right goal, median =
757 0.22 Hz vs control zone, median = 0.12 Hz, Mann–Whitney $U = 1266$, $p = .0012$; left goal,
758 median = 0.33 Hz vs control zone, median = 0.1 Hz, Mann–Whitney $U = 1108$, $p = .0009$).
759 The two goal zones were not combined as their firing was different (Mann–Whitney $U =$
760 1179, $p = .02$), however the firing of the two control zones was not different (Mann–Whitney U
761 = 2005, $p = .62$). In the case of speeds higher than 15 cm/s, i.e. when the rat was just
762 crossing the zones without stopping, there was no difference between the out-of-field firing at
763 goals (median = 0.12 Hz) and non-goals (median = 0.1 Hz, Mann–Whitney $U = 3569$, $p =$
764 .21; the firing at both goals or non-goals was not different and combined). Thus, goal-related
765 activity, i.e. out-of-field firing at the goal, seems to be expressed only at low speeds,
766 presumably during the waiting period. This result was reproduced when looking separately at

767 CA1 and, importantly, CA3 place cells: goal-related activity was present in both cases (for 55
768 CA1 place cells, median goals = 0.3 Hz, median at control zones = 0.18 Hz, Mann-Whitney U
769 = 1100, $p = .014$; for $n = 38$ CA3 place cells, median at goals = 0.29 Hz, median at control
770 zones = 0.08 Hz, Mann-Whitney $U = 377$, $p = .01$). Thus, we reproduce the goal-related
771 finding of the single goal version of the task (Hok et al., 2007a) and extend it to CA3 place
772 cells. Finally, we tested whether goal-related activity, for place cells without a field on any of
773 the goal zones ($n = 26$), had a bias towards a specific goal. To do so, we computed the side
774 firing preference index in 1vs1 sessions: its median was 0.05 and the distribution was
775 symmetric around 0 (Wilcoxon signed-rank test, $T = 138.5$, $p = .35$). Thus, both goals were
776 homogeneously represented.

777 *Temporal characteristics of activity during the delay period in the equal-value condition*

778 We then aimed to describe the temporal aspects of the goal activity and to evaluate possible
779 time coding during the goal delay period. For this, we combined the CA1 and CA3 data and
780 looked at the activity before (-4:-2s), during (-2:0) and after (0:2s) the delay at the goal, $t=0$
781 being the pellet dispenser actuation. Only sessions with at least 1 visit to each goal were
782 included in this analysis. Examples of raster plots and normalized peri-event time histograms
783 (PETHs) from 2 place cells are shown in Figure 6A. Individual PETHs were then averaged
784 over all place cells with no field or any of the goal zones ($n = 26$), shown in Figure 6B for
785 each goal separately (top). As observed in previous 1-goal versions of the task, the averaged
786 PETHs at the goal showed a drop upon entry in the goal and then an increase of firing
787 around 1s after entry in the zone. The population activity at the goal tends to reach its peak
788 after 1 s spent in the goal zone, consistent with previous results (Hok et al., 2007a). We first
789 compared the activity profile of the two goals and they were not significantly different
790 (Kolmogorov-Smirnov $D = 0.13$, $p = .62$). Thus, we combined the PETHs from the two goals
791 and compared the normalized firing rate during the first and second halves of the delay. The
792 firing rate significantly increased during the delay (median [-2: -1] = 0.23, median [-1: 0] =

793 0.65, paired Wilcoxon test, $W = 4$, $p = 1.3 \times 10^{-5}$). Finally, we performed the same comparison
794 when all place cells were taken together ($n = 101$) regardless of place field position. In that
795 case, the left and right distribution were different (Kolmogorov-Smirnov $D = 0.38$, $p = .0002$)
796 but the same increase during the delay was found, for the left goal (median [-2: -1] = 0.26,
797 median [-1: 0] = 0.57, paired Wilcoxon test, $W = 710.5$, $p = 7.33 \times 10^{-10}$) or the right goal (med
798 [-2: -1] = 0.36, med [-1: 0] = 0.57, paired Wilcoxon test, $W = 1206$, $p = 1.55 \times 10^{-5}$).
799 Incidentally, we also looked at the temporal profile around the reward consumption event
800 (which could take place anywhere in the arena): in contrast with firing during the goal period,
801 no notable variations in the firing of place cells were observed, whether all firing or only out-
802 of-field firing was considered (data not shown). Thus, the activity of place cells is temporally
803 organized during the goal delay, increasing as the rat waits at the goal.

804

805

Insert Fig. 6 near here

806

807 We also looked for evidence of temporally organized firing peaks representing the whole of
808 the 2s waiting period, consistent with previous reports of 'time cells' in the hippocampus
809 (MacDonald et al., 2011). To this end, we smoothed the PETH bins for each cell (bins = 0.1
810 s, Gaussian filter of sigma = 0.15 s) and computed the time of maximum firing, for each cell
811 and goal separately, during the 2s goal delay. Time coding would imply a reproducible
812 activity at specific times during the delay, whenever the animal was waiting at that goal. We
813 tested this for out-of-field firing and for place field firing, separately. For the out-of-field firing,
814 we could compare the repeatability of the order of firing at the left vs. the right goal. For place
815 field firing, we compared it across days for several recordings of the same cell. First, we
816 organized the individual PETHs of cells by their time of peak during the goal delay, including
817 only the cells whose normalized out-of-field firing PETH had a peak during the goal period
818 which was higher than 0.3. This ranking revealed a rather continuous representation of all
819 times during the delay period (see Figure 6D, top left, for the out-of-field firing at the left goal

820 during a daily 1vs1 session). However, imposing the cell order for one goal on the other goal
821 (data not shown) disrupted the temporal order of the neurons, indicating that if cells encode a
822 specific time with their out-of-field firing, it is different for the two goals (possible 'retiming' of
823 the cells, see MacDonald et al., 2011). To quantify this, we computed the correlation
824 between the order of cell numbers (from 1 to n) and the time of peak (in bins from the start).
825 The correlation for the left goal, setting the order of cells, was high as expected ($r(7) = 0.95$,
826 $p = 8.1 \times 10^{-5}$) but non-significant when the same order was applied to the other goal ($r(7) = -$
827 0.08 , $p = .8$). Thus, activity at the goal might seem to show peaks at all times during the
828 delay, but the time of the peaks is not consistent between goals, even though the delay at
829 both goals is always the same. This may reflect spatial inconstancy during this waiting
830 period, as the animal could still move around within the goal zone.

831 To test this further and assess place fields as well, we asked whether the temporal order of
832 firing was conserved between days. We compared the order of goal firing peaks between two
833 1vs1 sessions from different days where the same cells were recorded (sessions might differ
834 for each cell, but are termed 'Day 1' and 'Day 2' for simplicity). First, we analyzed the activity
835 of cells with a field at the goal (see Figure 6C for the left goal cells). For the left goal, the
836 correlation between cell order and time of maximum firing was significant on day 1 but not
837 day 2 ($n = 11$, $p = 2.3 \times 10^{-7}$ and $p = .95$ respectively), similar results were obtained for the right
838 goal ($n = 10$, $p = 6.5 \times 10^{-5}$ and $p = .53$). This same pattern of results was observed for cells
839 with no field on the goal in question (left goal out-of-field firing is shown in Figure 6D, left, $n =$
840 13 , $p = 6.1 \times 10^{-11}$ and $p = .64$, right, $n = 11$, $p = 8.3 \times 10^{-8}$ and $p = .14$). To summarize, the
841 activity of place cells at the goal is temporally organized insofar as firing increases around 1s
842 during the goal delay, but we do not see evidence of consistent, homogeneous time coding.

843 *Goal value coding?*

844 Next, we focused on the conditions with different values, to assess if hippocampal cells
845 encode the value of spatial goals in this task (see Figure 4 for an example of the activity of

846 several cells in the different value conditions). We decided to address this question with three
847 approaches. First, at the population level we asked whether place fields would change their
848 activity depending on goal values (by shifting their location, modulating their firing rate or via
849 changes of moment-to-moment firing). Second, we analyzed out-of-field goal firing to see
850 whether it would globally increase or decrease for a specific goal value. Third, at the single
851 cell level, we tested whether individual place cells with a field on the goal would consistently
852 encode specific goal values (out-of-field firing is individually too sparse to be analyzed per
853 cell).

854 First, to assess whether value-changing sessions would trigger remapping or field instability,
855 we computed the correlation, for each cell, between each session and all the subsequent
856 ones, either for this day or the other days where this cell was recorded. The average
857 correlation coefficient over all cells and sessions was 0.7 ± 0.085 (standard deviation),
858 hence, maps were overall very stable (min = 0.45, max = 0.80). The average correlation
859 between the first equal value session and all subsequent value-changing sessions was 0.69
860 ± 0.02 and the average correlation between the first equal-value session and all subsequent
861 equal-value sessions was also 0.69 ± 0.02 . Thus, there was no difference in the stability of
862 place cells between equal-value or value-changing sessions. Overall, we did not detect any
863 visible pattern linked to value-changing sessions (data not shown, but see examples in
864 Figure 4). So, general place cell activity was very stable **spatially** across sessions,
865 regardless of changes in goal value.

866 The place fields' COMs were computed for both types of value-changing sessions and their
867 spatial distribution is shown in Figure 7A. Using the same shuffle analysis as previously (see
868 methods), we assessed whether COMs inside or closest to the high-value goal were more
869 numerous than COMs inside or closest to any of the control zones or to the other, lower-
870 value, goal. None of the value configurations exhibited any form of goal inhomogeneity (cf.
871 Figure 7A).

872 Next, we asked whether place cells would encode goal value via modulations of their place
873 field firing rate. We comparing firing rates at the high-value goals to those in the low-value
874 goals, including only data when a place field was encroaching on a given zone. This is
875 illustrated by the cumulated rate maps for all recorded place cells shown in Figure 7B. For
876 both value configurations, cells fired similarly in the low and high value goal zones (1vs0,
877 low-goal vs high-goal Mann–Whitney $U = 2092$, $p = .70$; 1vs3, low-goal vs high-goal Mann–
878 Whitney $U = 1613$, $p = .90$), see Figure 7C. The same comparison yielded similar results
879 when restricted to low or high speed data (data not shown).

880 Lastly, we sought a way to analyze the trial-to-trial variability of place cells' firing in the
881 different value conditions to assess whether, even though place fields appeared very stable,
882 there could be more subtle variations in firing between equal value and value-changing
883 conditions. The overdispersion measure allows to quantify this as the variability of the firing
884 of a place cell across several passes through its place field. First, to compare our results to
885 the existing literature, we computed the overdispersion of the population of place cells
886 recorded in each condition using the method of (Fenton et al., 2010). We found that the
887 overdispersion in the 1vs1 condition was 3.42 (Figure 7D, left), which is very similar to values
888 observed in comparable tasks in the literature (Fenton et al., 2010; Hok et al., 2013).
889 Interestingly, we also obtained very similar values in the value-changing conditions (Figure
890 7D middle and right): the overdispersion was 3.19 for 1vs0 and 3.23 for 1vs3. To assess
891 whether there could be an effect of goal value changes on the overdispersion of individual
892 place cells, we performed the overdispersion computation on individual cells. To obtain a
893 sufficiently accurate estimate of overdispersion (which is the variance of the distribution of z-
894 values for each pass through the place field), we only used place cells that provided at least
895 20 passes. We first compared the overdispersion of CA1 and CA3 place cells and found no
896 difference between these two populations in any of the conditions (1vs1, 1vs0 or 1vs3, data
897 not shown); thus, CA1 and CA3 place cells were combined for the rest of the analysis. We
898 then used a paired design comparing the overdispersion for value-changing sessions to that

899 of the corresponding (i.e., for the same cell and day) equal-value session. In the 1vs0
900 condition, there was no difference of overdispersion when compared to the corresponding
901 1vs1 sessions (med 1vs1 = 2.6, med 1vs0 = 2.4, paired Wilcoxon signed-rank test, $T = 391$,
902 $p = .10$ for $n = 46$ place cells). Similarly, no difference was found between 1vs3 sessions and
903 the corresponding 1vs1 sessions (med 1vs1 = 2.4, med 1vs3 = 2.6, paired Wilcoxon signed-
904 rank test, $T = 448$, $p = .15$ for $n = 48$ place cells). This analysis included all place cells, while
905 perhaps only the cells with a place field close to the goal with a changing value would be
906 affected by the change. We repeated the analysis using only cells with a place field on the
907 changing-value goal ($n = 24$ cells for 1vs0, $n = 27$ cells for 1vs3). The same results were
908 observed: there was no significant effect of changing the goal value on the overdispersion of
909 place cells (med 1vs1 = 2.8, med 1vs0 = 2.9, paired Wilcoxon signed-rank test, $T = 140$, $p =$
910 $.78$ for $n = 24$ place cells; med 1vs1 = 2.7, med 1vs3 = 2.9, paired Wilcoxon signed-rank test,
911 $T = 179$, $p = .81$ for $n = 27$ place cells). In conclusion, the overdispersion of place cells does
912 not significantly change between different value conditions. This is possibly in contrast with a
913 report from Wikenheiser and Redish (2011), where changes in reward contingencies
914 modulated the overdispersion; however, in this task the change in reward contingency
915 probably modified the strategy to use (always skip a goal instead of stopping at each goal)
916 and the differences in overdispersion could be due to this change of strategy, possibly
917 related to changes in spatial attention.

918

919

Insert Fig. 7 near here

920

921 Next, we addressed the question of value coding by the out of field firing of place cells. To do
922 so, we combined CA1 and CA3 data and first focused on the firing at the two goals of
923 different value in all the speed conditions (see Figure 7E for low speeds). Even though
924 significant goal firing had been found in the 1vs1 condition for low speeds, there was no
925 difference between the firing rate at high-value goals versus low-value goals in the 1vs0

926 condition ($n = 104$ cells, Mann–Whitney $U = 5249$, $p = .70$) nor in the 1vs3 condition ($n = 92$
927 cells, Mann–Whitney $U = 3727$, $p = .20$). As another approach to assess a possible value
928 coding of goal-related activity, we computed the value firing preference index (see Methods).
929 This only included place cells with no place field at any of the goals. The median value firing
930 preference index was <0.001 in 1vs0 conditions ($n = 24$ place cells) and was not different
931 from 0 (Wilcoxon signed-rank test, $T = 120$, $p = .39$), indicating that cells were not firing more
932 at any of the goals (in particular, the firing did not increase for the high-value goals).
933 Similarly, the median index was -0.06 in the 1vs3 condition ($n = 19$ place cells) which was not
934 different from 0 (Wilcoxon signed-rank test, $T = 74$, $p = .39$). Thus, the goal firing was not
935 biased towards a specific goal value. Overall, neither place fields nor out-of-field activity
936 encoded goal value at the population level, indicating that goal-related activity in particular is
937 unlikely to be reflecting reward expectation.

938 PETH data – We next asked whether the temporal profile of out-of-field goal-firing would be
939 different depending on goal value. Focusing first on cells with no place field at either of the
940 goals, low vs high value PETHs for the 1vs0 condition ($n = 24$) yielded a significant difference
941 over the whole PETH period (Kolmogorov-Smirnov $D = 0.33$, $p = .0018$) but no difference
942 was observed in the 1vs3 condition ($n = 19$, Kolmogorov-Smirnov $D = 0.09$, $p = .90$).
943 Focusing on the 1vs0 condition, in both goal zones neurons increased their firing rate during
944 the second half of the delay period ($t(23) = -7.9$, $p = 4.8 \times 10^{-8}$, $t(23) = -8.1$, $p = 3.8 \times 10^{-8}$,
945 respective paired t-tests), reproducing the results for the 1vs1 condition. Also for the 1vs0
946 condition, in the one pellet goal zone, neurons decreased their firing rate as the rat exited the
947 zone (normalized firing rate for $[-1s:0s] = 0.68 \pm 0.3$, for $[0s:1s] = 0.32 \pm 0.2$, $t(23) = 5.6$, $p =$
948 9.6×10^{-6} , paired t-test). In the goal zone yielding no pellets, this same decrease was present,
949 but of visibly smaller amplitude (see Figure 7F, top left; normalized firing rate for $[-1s:0s] =$
950 0.6 ± 0.3 , for $[0s:1s] = 0.47 \pm 0.3$, $t(23) = 67$, $p = .03$, paired t-test). A possible explanation for
951 this could be the absence of the pellet dispenser sound at the end of the unrewarded delay
952 period. This is only of interest if one focuses on the activity outside of the delay period, which

953 we did not aim to do, but could indicate sustained goal-firing. Overall, the analysis of goal-
954 related activity PETHs from the value-changing conditions confirms the increase in overall
955 firing during the delay period, regardless of goal value, and possibly suggests some influence
956 of the absence of expected reward on the temporal profile of goal-related activity.

957 Single-cell analysis – Finally, we aimed to investigate further if value-coding was completely
958 absent from the place cell population by focusing on individual cells. We compared, in each
959 condition (1vs0 or 1vs3) and for each goal (left or right) separately, the firing rate for that goal
960 when value was changed to its firing rate in the preceding reference session. To do so, we
961 computed the firing preference index between goals visited at least 5 times in the sessions of
962 interest. The firing preference index was statistically tested against a shuffled distribution of
963 the same data (see Methods). The results were evaluated in two ways. First, we labelled a
964 cell as ‘transiently value-modulated’ if it had at least one instance of value coding, whether
965 positively (higher firing in the value condition) or negatively (lower firing in the value
966 condition). We found that 25 % (n = 32) of place cells recorded in the 1vs3 condition were
967 “transiently value-modulated”, as were 17.5 % (n = 29) of place cells recorded in the 1vs0
968 condition. When CA1 and CA3 place cells were considered separately, the proportions of
969 ‘transiently value-modulated’ cells were similar (in 1vs3, 24 % for CA1, 26 % for CA3; in
970 1vs0, 14 % for CA1, 23.5 % for CA3). Then, we considered that a ‘true’ value-coding cell, as
971 for a place cell, would have to consistently encode goal value. Thus, we labelled cells as
972 ‘consistently value-coding’ if they coded value in the same way (i.e. either by a significant
973 increase or decrease of firing rate) for more than half of the instances in which this cell had
974 been recorded in the same value condition. 29 repeatedly recorded place cells were
975 analyzed either for 1vs3 (18 CA1 place cells, 11 CA3 place cells) or 1vs0 sessions (17 CA1,
976 12 CA3 place cells). None of the 29 place cells tested were consistently value-coding in any
977 of the conditions.

978 Thus, in our task, place cells sometimes increased or decreased their firing following a
979 change in goal value, in individual sessions, in similar proportions to what was previously
980 reported in tasks with less spatial demands (in CA1, Lee et al., 2012b, in CA1 and CA3,
981 2017, Tryon et al., 2017). However, this could be due to global fluctuations of firing rate
982 independent from goal value, as individual cells did not consistently encode the value of the
983 goals. Overall, when individual and population results are taken together, place cells do not
984 encode goal value in our paradigm.

985 *Local Field Potential (LFP) – theta rhythm at the goal*

986 Finally, we focused on hippocampal theta (4-12 Hz) and analyzed its power and frequency at
987 the goal, first in the equal-value conditions, then in the modified value conditions. An
988 example of theta power density estimate is shown in Figure 8A. The left goal theta power
989 (median = 25.5) did not differ from the right goal theta power (median = 25.3, Wilcoxon
990 signed rank test, $Z = 0.01$, $p = .9$) and the theta frequency at the left goal (median = 7.8 Hz)
991 did not differ from that of the right goal (median = 7.9 Hz, Wilcoxon signed rank test, $Z = -1.3$,
992 $p = .19$), so the two sides were combined. Figure 8B shows the power spectral density
993 estimates just before goal zone entry (-4 to -2s) and during the goal delay (-2 to 0s), for the
994 two goals combined, averaged over all 1vs1 sessions. The power and frequency of the theta
995 rhythm decreased during the goal delay period (-4:-2s), median power = 7.8, median
996 frequency = 7.8 Hz, compared to pre-goal period (-2:0s), median power = 26.4, median
997 frequency = 8.3 Hz, Wilcoxon on power, $Z = 12.7$, $p = 2.4 \times 10^{-37}$; Wilcoxon on frequency, Z
998 = 9.3, $p = 1.9 \times 10^{-20}$). Thus, theta power and frequency both decreased significantly in the
999 goal zone compared to the previous 2 seconds, as was observed in the single-goal version
1000 of the task (Hok et al., 2007a).

1001

1002

1003

Insert Fig. 8 near here

1004 Our paradigm allows the comparison of theta parameters for very similar behaviors when the
1005 rat is expecting different amounts of reward (cf. Figure 8 D and E). Comparing theta power
1006 between the different value conditions (whether for 1vs0 or 1vs3 sessions) did not show any
1007 significant difference (low vs high goal for 1vs0, Wilcoxon $Z = -0.8$, $p = .40$; low vs high goal
1008 for 1vs3, Wilcoxon $Z = -0.51$, $p = .60$). However, the theta frequency was significantly
1009 different between the low and high-value goal, but only for 1vs0 sessions (low-value goal
1010 median = 7.9 Hz, high-value goal median = 7.7 Hz, Wilcoxon $Z = 5.6$, $p = 1.9 \times 10^{-8}$). For 1vs3
1011 sessions, theta frequencies at the two goals were not different (Wilcoxon $Z = 0.36$, $p = .72$).

1012 Overall, the results from the LFP analysis show correlates with running speed. There were
1013 no consistent differences evident as a function of expected or actual reward value, even
1014 though behaviorally the rats distinguished the goal types. The only difference observed,
1015 namely, between goals providing 1 or 0 pellet, might require some more investigation, as a
1016 subtle difference in that condition is also observed in the hippocampal cells' PETHs profile.
1017 The only difference during the goal period between the 0 value condition and the others,
1018 aside for the difference in value, is that the next action of the rat should be to go to the other
1019 goal, instead of exploring the arena for food. Perhaps rats in that condition are anticipating or
1020 planning a different type of action/trajectory and this might contribute to the subtle differences
1021 observed. Overall, our LFP results somewhat diverge from the recent findings of Tryon et al.
1022 (2017), who found effects of varying reward probability and other parameters such as agency
1023 on the theta rhythm; we suspect that these contrasting results arise from the differences in
1024 task demands.

1025 **Discussion**

1026 We investigated whether hippocampal place cells are sensitive to goal value, consistent with
1027 a role for hippocampus in goal-directed navigation. We show that rats can learn to navigate
1028 to either of two unmarked goal locations, and prefer the more rewarding goal. We replicated
1029 previous observations of out-of-field, goal-related activity from dorsal CA1 place cells (Hok et

1030 al., 2007a, 2007b, 2013; Hayashi et al., 2016) and extended these findings to CA3. However,
1031 place cells did not encode goal value, either with their place field or out-of-field firing. We
1032 conclude that, during flexible navigation, dorsal hippocampal place cells encode space in a
1033 value-free manner. These findings and conclusions are examined in detail, below.

1034 *Electrophysiological markers of goal encoding*

1035 Rats were able to navigate efficiently to the goals, and were also attuned to the 2s interval
1036 between reaching the goal zone and reward delivery (or absence thereof), demonstrating
1037 knowledge of the goal locations. Electrophysiologically, we first looked for evidence of goal
1038 encoding, since multiple studies have observed over-representation of goal locations by
1039 place fields (Hollup et al., 2001; Kobayashi et al., 2003; Lee et al., 2006; Dupret et al., 2010)
1040 or out-of-field firing (Hok et al., 2007a, 2007b, 2013; Hayashi et al., 2016).

1041 First, we did not see place fields clustered around the goals; this is similar to previous reports
1042 but stands in contrast to several other studies, for reasons that appear task-related. Tasks
1043 that seem least likely to elicit goal overrepresentation involve variable behavioral phases
1044 (e.g. goal-directed alternating with foraging), dissociate goal from reward location and/or
1045 involve multiple routes to the goal (Wiener et al., 1989; Speakman and O'Keefe, 1990;
1046 Markus et al., 1995; Gothard et al., 1996; Zinyuk et al., 2000; Jeffery et al., 2003; Anderson
1047 et al., 2006; Ainge et al., 2007, 2012, Hok et al., 2007a, 2007b; Grieves et al., 2016; Spiers
1048 et al., 2017). In contrast, goal over-representation by place fields has been observed in tasks
1049 that entail the use of repeated, overlapping trajectories, provide reward at the goal location,
1050 and may include a novelty aspect (Eichenbaum et al., 1987; Breese et al., 1989; Kobayashi
1051 et al., 1997, 2003; Hollup et al., 2001; Fyhn et al., 2002; Lee et al., 2006; Dupret et al., 2010;
1052 Lee et al, 2012b; McKenzie et al., 2013; Lee et al, 2017; Mamad et al., 2017; Tryon et al.,
1053 2017; Gauthier and Tank, 2018). Further research is clearly needed to untangle the role of
1054 these parameters.

1055 In contrast with the absence of place field clustering at goals, we found increased out-of-field
1056 population spiking at the goals, occurring when the rat was paused or moving very slowly,
1057 developing after around 1 s spent at the goal. This replicates previous findings from 1-goal
1058 versions of the continuous navigation task (Hok et al., 2007a, 2007b, 2013; Hayashi et al.,
1059 2016). Such activity has not been seen in tasks where animals did not have to wait at the
1060 goal (Zinyuk et al., 2000; Anderson et al., 2006) or waited with a shorter delay (Siegel et al.,
1061 2008). Moreover, goal-firing activity is attenuated and occurs earlier in a cued version (Hok et
1062 al., 2007a). Finally, we found that this firing was independent of goal value. Taken together,
1063 this suggests that the goal-firing may relate to parameters that are more spatial than
1064 motivational, for example, a confirmation that the current location is indeed a goal.

1065 Arguably, goal-related firing might be related to reactivation phenomena, such as theta
1066 sequences (Foster and Wilson, 2007), or sharp-wave/ripple (SWR) - related replay (Foster
1067 and Wilson, 2006; Pfeiffer and Foster, 2013). Theta sequences, which are sequential place
1068 cell firing events occurring within one or a few theta cycles, generally during running, might
1069 reflect route planning, as they have previously been found to extend towards goal locations
1070 (Wikenheiser and Redish, 2015). However, in our case the rat was *at* the goal during the
1071 expression of goal-firing, and its future route still unpredictable at this stage: thus, theta
1072 sequences could not contain relevant trajectory information. Firing during the goal waiting
1073 period is thus unlikely to be attributable to theta sequences. Alternatively, SWRs are known
1074 to co-occur during replay of place cell sequences, usually during pauses around the reward
1075 location. We think our data are unlikely to reflect SWRs for several reasons. First, in our
1076 previous study (Hok et al., 2007a), no SWRs were observed during the goal zone periods.
1077 Second, in a circular track task, waiting for reward at a goal was linked to a decrease of
1078 SWRs (McKenzie et al., 2013). Finally, reduced goal-firing in mutant mice was not found to
1079 be linked to reduced SWR activity at the goal (Hayashi et al., 2016). For these reasons, we
1080 did not attempt to optimize our setup for the artefact-free detection of SWRs. That said, we
1081 did look at the LFP data and did not see evidence of goal-related SWR activity (data not

1082 shown). Overall, it seems unlikely that goal-related firing could be an expression of SWR-
1083 related replay.

1084 *Electrophysiological markers of goal value*

1085 Our main result is that, while rats adapted their goal choices as a function of goal value,
1086 place cell activity was unaffected by changes in goal value. Place fields did not move
1087 towards the more (or less) rewarded locations, nor did they significantly change their pattern
1088 of firing as a function of goal value. The overdispersion of cells did not change between
1089 equal value or value-changing sessions and was generally low, similar to equivalent tasks
1090 with one goal of constant value. Goal firing did not increase at the low or high-value goal, and
1091 while a small proportion of individual cells transiently modulated their firing when goal value
1092 changed, this effect did not last over successive recordings of the same cell, in contrast to
1093 the stability of place cells' spatial firing. Relatively few studies have addressed the issue of
1094 value coding in the hippocampus. In the majority of these studies, reward consumption co-
1095 occurred with the spatial location of the goal, making it difficult to differentiate goal from
1096 reward. One such study, in agreement with ours, found no evidence of goal value encoding
1097 (i.e. number of water drops delivered at a location, Tabuchi et al., 2003). Other reports
1098 suggest that place cells may encode reward probability, action value, or reward expectation
1099 signals in linear mazes that did not require to locate a spatially-defined unmarked goal (Lee
1100 et al., 2012b, Lee et al., 2017; Tryon et al., 2017). Goal value findings in these studies might
1101 instead relate to emotional enhancement of firing. For example, in a study by Tryon et al.
1102 (2017), rats had to choose between left and right doors on a forked linear maze, which
1103 provided either a low reward with 100% probability, or a high reward with variable probability.
1104 Place cells fired more for the lowest probability (12.5%) choice but only when reward was
1105 going to be delivered. One explanation for this could be that the occurrence of an
1106 unexpected reward triggers neurochemical reward signals ("surprised pleasure"). Our study,
1107 by contrast, mostly focused on the period before choice feedback was available and

1108 dissociated goal and reward locations; in that case, no goal value encoding was found in the
1109 activity of place cells. Tryon et al. (2017) also found that reward probability and other task
1110 variables influenced theta power. In our paradigm, only trials where the rat waited at the 0-
1111 pellet goal yielded subtle electrophysiological differences, in the form of a blunted firing
1112 profile during the latter half of the delay, or a lower theta frequency; these might also reflect
1113 emotional responses to the realization that reward would not follow. Finally, the hippocampus
1114 might encode goal value via modulations of place cell reactivations (either theta sequences
1115 or ripple-related replay, see Ambrose et al., 2016) or other phenomena that the present study
1116 did not address (e.g. phase precession). Future studies will need to combine large-scale
1117 recordings with a spatial task to assess whether these parameters might encode the value of
1118 a spatial goal; such a result would be especially surprising given that individual place cells do
1119 not appear to encode goal value.

1120 Overall, the idea that place cells are coding space independently from value is in line with the
1121 theory of a predominantly spatial cognitive map (O'Keefe and Nadel, 1978). Neurons
1122 encoding goals, their value, or different decision-making parameters such as reward
1123 expectation have been found in other brain regions (Doya, 2008); reviewing these reports
1124 goes beyond the scope of the present study, so we will focus on two regions that receive
1125 inputs from the hippocampus – the prefrontal cortex and the striatum. Goal cells or reward-
1126 related signals were found in the medial prefrontal cortex (Hok et al., 2005) and in the
1127 orbitofrontal cortex (Feierstein et al., 2006; Riceberg and Shapiro, 2017), for reviews see
1128 Wikenheiser and Schoenbaum (2016), Grieves and Jeffery (2017) and Poucet and Hok
1129 (2017). Additionally, the striatum is involved in reward processing, expected outcome coding
1130 and possibly combining reward and place information (Lavoie and Mizumori, 1994; Lansink
1131 et al., 2009; Gmaz et al., 2018). It is thus likely that the hippocampus focuses on spatial
1132 encoding (in particular in a task requiring accurate spatial navigation) while other brain
1133 structures evaluate goal value and link this information with goal location.

1134

1135 *Conclusion*

1136 Our results suggest that, in an open-field arena with high navigation demands and low route
1137 stereotypy (high variability), place cells show evidence of goal-related activity but no
1138 evidence of goal *value* coding. What electrophysiological changes we did see may reflect
1139 neurochemical processing of reward expectation/anticipation, for which future studies of
1140 cellular excitability, as well as studies that assess the repeatability of the encoding of the
1141 phenomenon of interest, may be illuminating. Overall, our results support a predominantly
1142 spatial memory function for the rodent hippocampus and suggest that additional features of
1143 an environment, such as the value of specific places, are added to the ‘map’ by downstream
1144 structures.

1145 **List of references**

1146 Ahmed OJ, Mehta MR (2012) Running speed alters the frequency of hippocampal gamma
1147 oscillations. *J Neurosci* 32:7373–7383.

1148 Ainge JA, Tamosiunaite M, Woergötter F, Dudchenko PA (2007) Hippocampal CA1 place
1149 cells encode intended destination on a maze with multiple choice points. *J Neurosci*
1150 27:9769–9779.

1151 Ainge JA, Tamosiunaite M, Wörgötter F, Dudchenko PA (2012) Hippocampal place cells
1152 encode intended destination, and not a discriminative stimulus, in a conditional T-maze
1153 task. *Hippocampus* 22:534–543.

1154 Alexander GM, Farris S, Pirone JR, Zheng C, Colgin LL, Dudek SM (2016) Social and novel
1155 contexts modify hippocampal CA2 representations of space. *Nat Commun* 7:10300.

1156 Ambrose RE, Pfeiffer BE, Foster DJ (2016) Reverse Replay of Hippocampal Place Cells Is

- 1157 Uniquely Modulated by Changing Reward. *Neuron* 91:1124–1136.
- 1158 Anderson MI, Killig S, Morris C, O'Donoghue A, Onyiaha D, Stevenson R, Verriotis M,
1159 Jeffery KJ (2006) Behavioral correlates of the distributed coding of spatial context.
1160 *Hippocampus* 16:730–742.
- 1161 Bendor D, Wilson MA (2012) Biasing the content of hippocampal replay during sleep. *Nat*
1162 *Neurosci* 15:1439–1444.
- 1163 Bokil H, Andrews P, Kulkarni JE, Mehta S, Mitra PP (2010) Chronux: A platform for analyzing
1164 neural signals. *J Neurosci Methods* 192:146–151.
- 1165 Brandon MP, Koenig J, Leutgeb JK, Leutgeb S (2014) New and Distinct Hippocampal Place
1166 Codes Are Generated in a New Environment during Septal Inactivation. *Neuron* 82:789–
1167 796.
- 1168 Breese CR, Hampson RE, Deadwyler SA (1989) Hippocampal place cells: stereotypy and
1169 plasticity. *J Neurosci* 9:1097–1111.
- 1170 Diamantaki M, Coletta S, Nasr K, Zeraati R, Laturus S, Berens P, Preston-Ferrer P,
1171 Burgalossi A (2018) Manipulating Hippocampal Place Cell Activity by Single-Cell
1172 Stimulation in Freely Moving Mice. *Cell Rep* 23:32–38.
- 1173 Donnelly NA, Holtzman T, Rich PD, Nevado-Holgado AJ, Fernando ABP, Van Dijck G,
1174 Holzhammer T, Paul O, Ruther P, Paulsen O, Robbins TW, Dalley JW (2014)
1175 Oscillatory activity in the medial prefrontal cortex and nucleus accumbens correlates
1176 with impulsivity and reward outcome. *PLoS One* 9.
- 1177 Doya K (2008) Modulators of decision making. *Nat Neurosci* 11:410–416.
- 1178 Dupret D, O'Neill J, Pleydell-Bouverie B, Csicsvari J (2010) The reorganization and
1179 reactivation of hippocampal maps predict spatial memory performance. *Nat Neurosci*
48

- 1180 13:995–1002.
- 1181 Eichenbaum H, Kuperstein M, Fagan A, Nagode J (1987) Cue-sampling and goal-approach
1182 correlates of hippocampal unit activity in rats performing an odor-discrimination task.
1183 *JNeurosci* 7:716–732.
- 1184 Epsztein J, Brecht M, Lee AKK (2011) Intracellular determinants of hippocampal CA1 place
1185 and silent cell activity in a novel environment. *Neuron* 70:109–120.
- 1186 Feierstein CE, Quirk MC, Uchida N, Sosulski DL, Mainen ZF (2006) Representation of
1187 Spatial Goals in Rat Orbitofrontal Cortex. *Neuron* 51:495–507.
- 1188 Fenton AA, Lytton WW, Barry JM, Lenck-Santini P-P, Zinyuk LE, Kubík S, Bures J, Poucet B,
1189 Muller RU, Olypher A V (2010) Attention-like modulation of hippocampus place cell
1190 discharge. *J Neurosci* 30:4613–4625.
- 1191 Foster DJ, Wilson MA (2006) Reverse replay of behavioural sequences in hippocampal place
1192 cells during the awake state. *Nature* 440:680–683.
- 1193 Foster DJ, Wilson MA (2007) Hippocampal theta sequences. *Hippocampus* 17:1093–1099.
- 1194 Fyhn M, Molden S, Hollup S, Moser M-B, Moser EI (2002) Hippocampal Neurons
1195 Responding to First-Time Dislocation of a Target Object. *Neuron* 35:555–566.
- 1196 Gauthier JL, Tank DW (2018) A Dedicated Population for Reward Coding in the
1197 Hippocampus. *Neuron* 99:179–193.e7.
- 1198 Gmaz JM, Carmichael JE, van der Meer MA (2018) Persistent coding of outcome-predictive
1199 cue features in the rat nucleus accumbens. *Elife* 7.
- 1200 Gothard KM, Skaggs WE, McNaughton BL (1996) Dynamics of Mismatch Correction in the
1201 Hippocampal Ensemble Code for Space: Interaction between Path Integration and

- 1202 Environmental Cues. *J Neurosci* 16:8027–8040.
- 1203 Grieves RM, Jeffery KJ (2017) The representation of space in the brain. *Behav Processes*
1204 135:113–131.
- 1205 Grieves RM, Wood ER, Dudchenko PA (2016) Place cells on a maze encode routes rather
1206 than destinations. *Elife* 5.
- 1207 Hartigan JA, Hartigan PM (1985) The Dip Test of Unimodality. *Ann Stat* 13:70–84.
- 1208 Hayashi Y, Sawa A, Hikida T (2016) Impaired hippocampal activity at the goal zone on the
1209 place preference task in a DISC1 mouse model. *Neurosci Res* 106:70–73.
- 1210 Hok V, Chah E, Save E, Poucet B (2013) Prefrontal cortex focally modulates hippocampal
1211 place cell firing patterns. *J Neurosci* 33:3443–3451.
- 1212 Hok V, Lenck-Santini P-P, Roux S, Save E, Muller RU, Poucet B (2007a) Goal-related
1213 activity in hippocampal place cells. *J Neurosci* 27:472–482.
- 1214 Hok V, Lenck-Santini P-P, Save E, Gaussier P, Banquet JP, Poucet B (2007b) A test of the
1215 time estimation hypothesis of place cell goal-related activity. *J Integr Neurosci* 6:367–
1216 378.
- 1217 Hok V, Save E, Lenck-Santini PP, Poucet B (2005) Coding for spatial goals in the
1218 prelimbic/infralimbic area of the rat frontal cortex. *Proc Natl Acad Sci U S A* 102:4602–
1219 4607.
- 1220 Hollup SA, Molden S, Donnett JG, Moser MB, Moser EI (2001) Accumulation of hippocampal
1221 place fields at the goal location in an annular watermaze task. *J Neurosci* 21:1635–
1222 1644.
- 1223 Jeffery KJ, Gilbert A, Burton S, Strudwick A (2003) Preserved performance in a hippocampal

- 1224 dependent spatial task despite complete place cell remapping. *Hippocampus* 13:175–
1225 189.
- 1226 Kobayashi T, Nishijo H, Fukuda M, Bures J, Ono T (1997a) Task-dependent representations
1227 in rat hippocampal place neurons. *J Neurophysiol* 78:597–613.
- 1228 Kobayashi T, Nishijo H, Fukuda M, Bures J, Ono T (1997b) Task-Dependent
1229 Representations in Rat Hippocampal Place Neurons. *J Neurophysiol* 78:597–613.
- 1230 Kobayashi T, Tran AH, Nishijo H, Ono T, Matsumoto G (2003) Contribution of hippocampal
1231 place cell activity to learning and formation of goal-directed navigation in rats.
1232 *Neuroscience* 117:1025–1035.
- 1233 Lansink CS, Goltstein PM, Lankelma J V., McNaughton BL, Pennartz CMA (2009)
1234 Hippocampus Leads Ventral Striatum in Replay of Place-Reward Information Stevens
1235 CF, ed. *PLoS Biol* 7:e1000173.
- 1236 Lavoie AM, Mizumori SJY (1994) Spatial, movement- and reward-sensitive discharge by
1237 medial ventral striatum neurons of rats. *Brain Res* 638:157–168.
- 1238 Lee D, Lin B-J, Lee AK (2012a) Hippocampal Place Fields Emerge upon Single-Cell
1239 Manipulation of Excitability During Behavior. *Science* (80-) 337:849–853.
- 1240 Lee H, Ghim J-W, Kim H, Lee D, Jung M (2012b) Hippocampal neural correlates for values
1241 of experienced events. *J Neurosci* 32:15053–15065.
- 1242 Lee I, Griffin AL, Zilli EA, Eichenbaum H, Hasselmo ME (2006) Gradual translocation of
1243 spatial correlates of neuronal firing in the hippocampus toward prospective reward
1244 locations. *Neuron* 51:639–650.
- 1245 Lee S-H, Huh N, Lee JW, Ghim J-W, Lee I, Jung MW (2017) Neural Signals Related to
1246 Outcome Evaluation Are Stronger in CA1 than CA3. *Front Neural Circuits* 11:40.

- 1247 MacDonald CJ, Lepage KQ, Eden UT, Eichenbaum H (2011) Hippocampal “Time Cells”
1248 Bridge the Gap in Memory for Discontiguous Events. *Neuron* 71:737–749.
- 1249 Mamad O, Stumpp L, McNamara HM, Ramakrishnan C, Deisseroth K, Reilly RB, Tsanov M
1250 (2017) Place field assembly distribution encodes preferred locations Csicsvari J, ed.
1251 *PLOS Biol* 15:e2002365.
- 1252 Markus EJ, Qin YL, Leonard B, Skaggs WE, McNaughton BL, Barnes CA (1995) Interactions
1253 between location and task affect the spatial and directional firing of hippocampal
1254 neurons. *J Neurosci* 15:7079–7094.
- 1255 McKenzie S, Robinson NTM, Herrera L, Churchill JC, Eichenbaum H (2013) Learning causes
1256 reorganization of neuronal firing patterns to represent related experiences within a
1257 hippocampal schema. *J Neurosci* 33:10243–10256.
- 1258 McNaughton BL, Barnes CA, O’Keefe J (1983) The contributions of position, direction, and
1259 velocity to single unit activity in the hippocampus of freely-moving rats. *ExpBrain Res*
1260 52:41–49.
- 1261 Morris RG, Garrud P, Rawlins JN, O’Keefe J (1982) Place navigation impaired in rats with
1262 hippocampal lesions. *Nature* 297:681–683.
- 1263 Moser EI, Kropff E, Moser MB (2008) Place cells, grid cells, and the brain’s spatial
1264 representation system. *AnnuRevNeurosci* 31:69–89.
- 1265 Moser MB, Moser EI, Forrest E, Andersen P, Morris RG (1995) Spatial learning with a
1266 minislab in the dorsal hippocampus. *Proc Natl Acad Sci* 92:9697–9701.
- 1267 Muller RU, Kubie JL, Ranck JB (1987) Spatial firing patterns of hippocampal complex-spike
1268 cells in a fixed environment. *J Neurosci* 7:1935–1950.
- 1269 Nishida H, Takahashi M, Lauwereyns J (2014) Within-session dynamics of theta–gamma
52

- 1270 coupling and high-frequency oscillations during spatial alternation in rat hippocampal
1271 area CA1. *Cogn Neurodyn* 8:363–372.
- 1272 O'Keefe J, Dostrovsky J (1971) The hippocampus as a spatial map. Preliminary evidence
1273 from unit activity in the freely-moving rat. *Brain Res* 34:171–175.
- 1274 O'Keefe J, Nadel L (1978) *The hippocampus as a cognitive map*. Clarendon Press.
- 1275 Park E, Dvorak D, Fenton AA (2011) Ensemble Place Codes in Hippocampus: CA1, CA3,
1276 and Dentate Gyrus Place Cells Have Multiple Place Fields in Large Environments
1277 Dickson CT, ed. *PLoS One* 6:e22349.
- 1278 Paxinos G, Watson C (2007) *The Rat Brain in Stereotaxic Coordinates Sixth Edition*.
1279 Academic Press Inc.
- 1280 Pfeiffer BE, Foster DJ (2013) Hippocampal place-cell sequences depict future paths to
1281 remembered goals. *Nature* 497:74–79.
- 1282 Poucet B, Hok V (2017) Remembering goal locations. *Curr Opin Behav Sci* 17:51–56.
- 1283 Powell NJ, Redish AD (2014) Complex neural codes in rat prelimbic cortex are stable across
1284 days on a spatial decision task. *Front Behav Neurosci* 8.
- 1285 Riceberg JS, Shapiro ML (2017) Orbitofrontal Cortex Signals Expected Outcomes with
1286 Predictive Codes When Stable Contingencies Promote the Integration of Reward
1287 History. *J Neurosci* 37:2010–2021.
- 1288 Rossier J, Kaminsky Y, Schenk F, Bures J (2000) The place preference task: a new tool for
1289 studying the relation between behavior and place cell activity in rats. *Behav Neurosci*
1290 114:273–284.
- 1291 Siegel JJ, Neunuebel JP, Knierim JJ (2008) Dominance of the Proximal Coordinate Frame in

- 1292 Determining the Locations of Hippocampal Place Cell Activity During Navigation. *J*
1293 *Neurophysiol* 99:60–76.
- 1294 Singer AC, Frank LM (2009) Rewarded Outcomes Enhance Reactivation of Experience in
1295 the Hippocampus. *Neuron* 64:910–921.
- 1296 Skaggs WE, McNaughton BL, Gothard KM, Markus EJ (1993) An information-theoretic
1297 approach to deciphering the hippocampal code. In. Citeseer.
- 1298 Speakman A, O'Keefe J (1990) Hippocampal Complex Spike Cells do not Change Their
1299 Place Fields if the Goal is Moved Within a Cue Controlled Environment. *Eur J Neurosci*
1300 2:544–555.
- 1301 Spiers HJ, Olafsdottir HF, Lever C (2017) Hippocampal CA1 activity correlated with the
1302 distance to the goal and navigation performance. *Hippocampus*.
- 1303 Tabuchi E, Mulder AB, Wiener SI (2003) Reward value invariant place responses and reward
1304 site associated activity in hippocampal neurons of behaving rats. *Hippocampus* 13:117–
1305 132.
- 1306 Tanaka KZ, He H, Tomar A, Niisato K, Huang AJY, McHugh TJ (2018) The hippocampal
1307 engram maps experience but not place. *Science* 361:392–397.
- 1308 Tanila H, Ku S, Kloosterman F, Wilson MA (2018) Characteristics of CA1 place fields in a
1309 complex maze with multiple choice points. *Hippocampus* 28:81–96.
- 1310 Thompson LT, Best PJ (1989) Place cells and silent cells in the hippocampus of freely-
1311 behaving rats. *J Neurosci* 9:2382–2390.
- 1312 Tolias AS, Ecker AS, Siapas AG, Hoenselaar A, Keliris GA, Logothetis NK (2007) Recording
1313 chronically from the same neurons in awake, behaving primates. *J Neurophysiol*
1314 98:3780–3790.

- 1315 Tolman EC (1948) Cognitive maps in rats and men. *Psychol Rev* 55:189–208.
- 1316 Trullier O, Shibata R, Mulder AB, Wiener SI (1999) Hippocampal neuronal position selectivity
1317 remains fixed to room cues only in rats alternating between place navigation and
1318 beacon approach tasks. *Eur J Neurosci* 11:4381–4388.
- 1319 Tryon VL, Penner MR, Heide SW, King HO, Larkin J, Mizumori SJYY (2017) Hippocampal
1320 neural activity reflects the economy of choices during goal-directed navigation.
1321 *Hippocampus* 27:743–758.
- 1322 Wiener SI (1993) Spatial and behavioral correlates of striatal neurons in rats performing a
1323 self-initiated navigation task. *J Neurosci* 13:3802–3817.
- 1324 Wiener SI, Paul CA, Eichenbaum H (1989) Spatial and behavioral correlates of hippocampal
1325 neuronal activity. *J Neurosci* 9:2737–2763.
- 1326 Wikenheiser AM, Redish AD (2011) Changes in reward contingency modulate the trial-to-trial
1327 variability of hippocampal place cells. *J Neurophysiol* 106:589–598.
- 1328 Wikenheiser AM, Redish AD (2015) Hippocampal theta sequences reflect current goals. *Nat*
1329 *Neurosci* 18:289–294.
- 1330 Wikenheiser AM, Schoenbaum G (2016) Over the river, through the woods: cognitive maps
1331 in the hippocampus and orbitofrontal cortex. *Nat Rev Neurosci* 17:513–523.
- 1332 Zinyuk L, Kubik S, Kaminsky Y, Fenton AA, Bures J (2000) Understanding hippocampal
1333 activity by using purposeful behavior: Place navigation induces place cell discharge in
1334 both task-relevant and task-irrelevant spatial reference frames. *Proc Natl Acad Sci*
1335 97:3771–3776.
- 1336

1337

1338 **Figure legends**

1339 **Figure 1** – Protocol and behavior in the 2-goal navigation task. (A) View of the task arena
1340 from above. (B) Task protocol. First, the rat navigates to one of the two goal zones,
1341 represented as small circles and corresponding to 20-cm of diameter unmarked zones
1342 located to the left or right of a white cue card. If the rat waits for 2s in a goal, a food pellet is
1343 released from an overhead dispenser and stops at a random location. Then, the rat leaves
1344 the goal to find and consume the food. The process repeats during 16-min sessions. (C)
1345 Example of two possible sequences of sessions; a specific sequence was performed on a
1346 given day, with no indication of change between its sessions. A control session was always
1347 performed first (equal rewards, 1:1), followed by a session with different values (e.g. 1:0,
1348 right goal unrewarded), then another control session (1:1) and finally the mirrored version of
1349 the first value session (e.g. 0:1, left goal unrewarded). On the next day, a sequence with the
1350 other set of goal values was usually performed (in 1:3 or 3:1, the right or left goal provides 3
1351 simultaneous pellets). (D) top, location of events from an example 1vs3 sequence. Reward
1352 consumption events are shown as crosses, correct (duration \geq 2s) goal visit events are
1353 shown as small circles. The number of recorded events of each type is shown at the right of
1354 each plot; the highest number of goal visits is underlined for each session. Note that reward
1355 locations appear randomly distributed in the environment and that goal events are
1356 concentrated on the goal zones (with rare occurrences of mistracked events). Bottom, timing
1357 of events from the same 1-3 sequence - raster marks at the top and bottom show left and
1358 right goal activation events, respectively. Cross marks show reward consumption events.
1359 The dotted line shows the side preference index of the rat towards the left or right (see
1360 Methods), computed in 1-min time bins. Note that the preference is approximately balanced
1361 in the first session, but switches towards the high-value goal on the 3:1 and 1:3 sessions,
1362 indicating sensitivity of the rat to the changing reward values. (E) Rat trajectory (top) and
1363 occupancy map (bottom) for the example sessions shown in D. The grey lines show the path

1364 of the rat; goals are shown as solid circles and control non-goal zones as dotted circles. The
1365 peak time for each occupancy map is shown in seconds.

1366 **Figure 2** – Behavior evidencing knowledge of the spatial, value and temporal aspects of the
1367 task. (A) Occupancy maps averaged across all sessions of a given type per rat and then
1368 across all 6 rats. Goals are indicated as plain circles while control zones are indicated with
1369 dotted circles, max bin value is indicated in seconds for each map. Note the increased time
1370 spent at the goals, specifically higher value ones. A slight preference for the right goal is
1371 visible in 1vs1 sessions, but this is only due to one rat and not significant. (B) Average time
1372 spent per session type in goal areas and control goal areas. Value-changing sessions of a
1373 given type (1:0 and 0:1, 1:3 and 3:1) were combined (into 1vs0 or 1vs3, respectively). The
1374 data from each are shown as individual dots and a boxplot is shown per condition (see
1375 Methods). Note the strong bias towards visiting the goal zones compared to control zones
1376 and the bias towards more valuable goals when appropriate. (C) Within-session development
1377 of the value preference index, computed over 1 min bins and averaged over sessions and
1378 then rats; preference for high value goal is shown for 1vs0 and 1vs3; spatial preference index
1379 is shown instead for 1vs1. Each point represents the average value for this bin and the
1380 shaded areas represent the standard error of the mean (s.e.m) across the 6 rats. The
1381 dashed line indicates no preference. Note the absence of clear side preference in equal
1382 value (1vs1) sessions and the rapid emergence of a preference for high value in value-
1383 changing (1vs0 and 1vs3) sessions. (D) Instantaneous speed profile around recorded reward
1384 consumption (top left) or goal activation events. For the reward consumption event, 0 is the
1385 time when the rat was seen eating a food pellet. Note the clear (but brief) speed decrease
1386 around this time. For goal events, the goal period is shown surrounded by two vertical lines
1387 (from -2 to 0s, 0 is the time of pellet dispenser activation). Note the increase of speed before
1388 arrival at the goal, the sharp decrease upon entry of the goal zone, the period of low-speed
1389 at the goal and finally the acceleration starting around the end of the delay period of 2s.

1390 Average speed during the goal delay did not differ between conditions. For all speed profiles,
1391 standard deviation across sessions is shown in grey and the scale is the same for all plots.

1392 **Figure 3** – Histology. Left, illustration of the estimated trajectory of the tetrode bundle for
1393 each rat. The verified coordinates of rat 32 were more anterior than planned (shown in inset).
1394 Right, example histology slice for the rat that provided the most cells in CA1 and position of
1395 the layers crossed by the tetrode track.

1396 **Figure 4** – The activity of place cells remains spatially stable when goal value changes. (A)
1397 Activity of 4 example place cells from CA1 that were recorded for at least two days in the
1398 1vs0 sequence and the 1vs3 sequence. The third session of each daily sequence (1:1) is not
1399 shown as it was not included in the analyses. Note that the order of the different sessions (or
1400 days) shown does not necessarily reflect the actual temporal order of the experiment (the
1401 position of the value-changing goal was counterbalanced between successive sessions of
1402 the same type as was the type of sequence). For a given cell, the spike plots (red spikes on
1403 grey trajectory) of each 16 min session are shown on the first row and the corresponding rate
1404 maps (average firing rate per bin, smoothed, with maximum firing rate indicated) are shown
1405 on the second row. Note how the rat behavior (visible on the spike plots) usually reflects goal
1406 values but how spatially stable the firing of the place cells remains within or across days,
1407 regardless of changes in goal value. This is the case even for place fields located on a goal
1408 (e.g. third cell from the top). Also note the often increased spiking at the goal zones (outside
1409 of place fields), which contributes to the population goal-related signal. (B) Example of a CA1
1410 place cell recorded during 4 different days, allowing for sampling of each value condition
1411 twice per goal. Spike and rate maps are shown as in A). Note the stability of the spatial firing
1412 across different value conditions. (C) Activity of 4 example place cells recorded during at
1413 least 2 days from CA3, presented as in A). (D) Example of a CA3 place cell recorded for 4
1414 different days, presented as in B). For CA3 cells too, changes in goal value do not appear to
1415 affect the firing of place cells.

1416 **Figure 5** – Place fields do not over-represent the goal locations in the equal-value (1vs1)
1417 condition (A) Distribution of the centers of mass (COMs) of all place fields in the 1vs1
1418 condition. Place fields were not significantly over-representing goal locations (black circles)
1419 compared to control zones (dashed circles). (B) For illustration purposes, cumulative firing
1420 map in the 1vs1 condition (average z-score in each location) using the z-scored speed-
1421 filtered map of each place cell. Note that firing rate does not seem to increase specifically at
1422 the goals. Average z-score is indicated. (C) Firing rate of place fields compared between
1423 goals and control non-goal zones, either for high-speeds (> 15 cm/s, left) or low-speed (< 15
1424 cm/s, right). Individual data points are shown as well as boxplots (which are as in Figure.
1425 2B). Place fields do not increase (nor decrease) their firing at the goals compared to the non-
1426 goals. (D) Correlations of all (smoothed) place cell maps at low vs high speed, compared to a
1427 shuffle distribution. The data are more correlated than chance and centered on high
1428 correlation values, hence, there is no global remapping between low speeds and high
1429 speeds. An example cell from CA3 is shown on the left. (E) Similar correlations as D but
1430 between goal-directed vs reward-search maps – with reward events shown as star markers
1431 and goal events shown as triangles. The example is from the same cell as in D. Again, the
1432 distribution of correlations from our data set are significantly higher than chance. Hence,
1433 there is no global remapping of place cells between these two task phases.

1434 **Figure 6** – Increase in out-of-field firing rate across the goal delay period and absence of
1435 time coding. (A) Left Example spike plot, raster plot and corresponding normalized peri-event
1436 time histogram (PETHs) for a CA1 cell recorded during a 1vs1 session, showing out-of-field
1437 activity at the left goal (and a place field on the right goal). The goal delay is shown by two
1438 vertical dashed lines. Right: Similar example but for a CA3 cell showing out-of-field activity
1439 on the right goal (and a place field on the left). (B) Temporal profile of goal-related activity
1440 (normalized firing during correct goal trials) for place cells with no field on any goal ($n = 26$),
1441 for the left and the right goal. The goal delay is indicated by the two vertical lines. Note the
1442 sharp decrease of firing upon entry in the goal zone, the increase during the delay period,

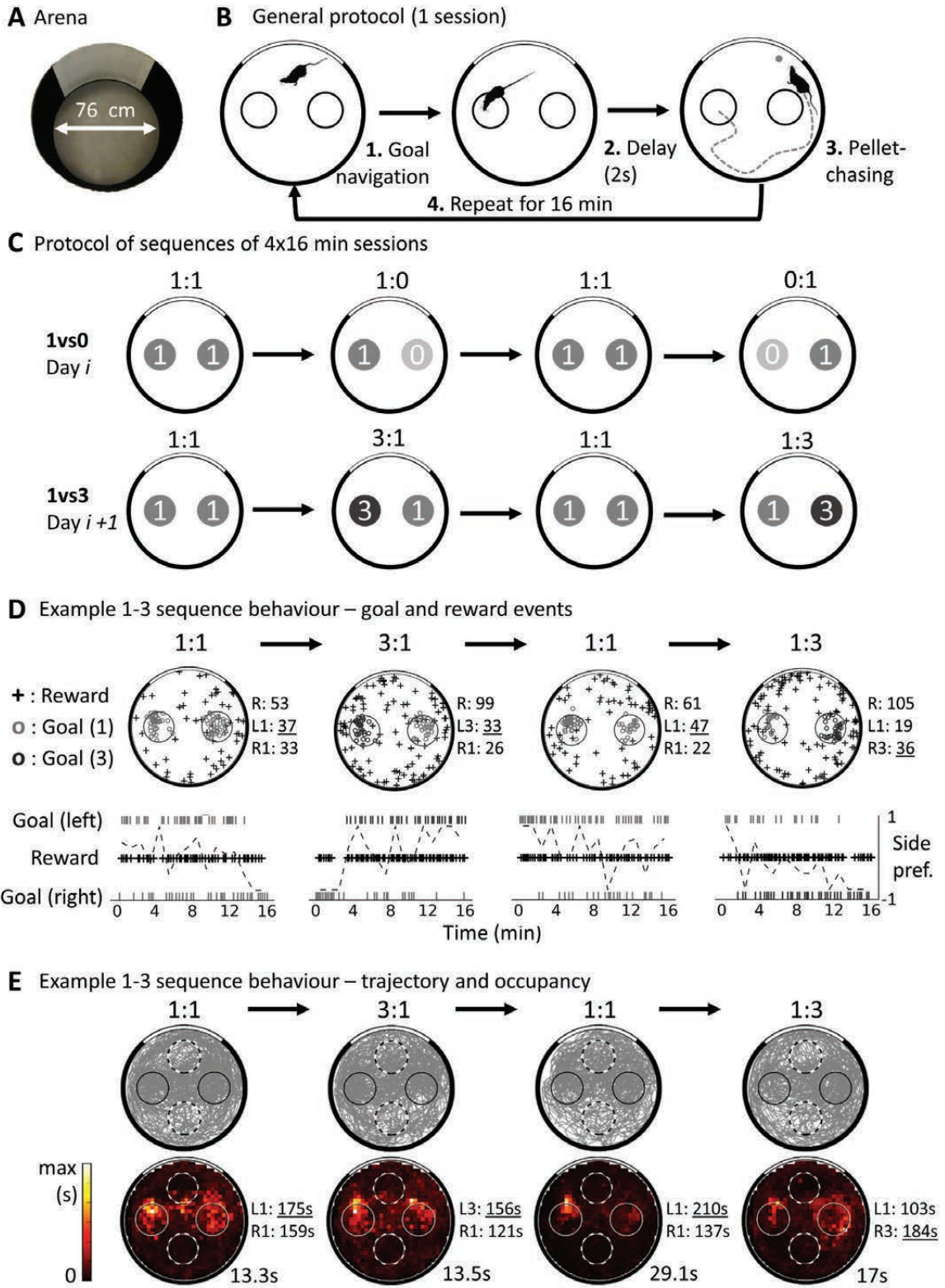
1443 followed by an abrupt drop just after the activation of the pellet dispenser. Shaded area =
1444 s.e.m. The corresponding average speed profile is shown below each plot. (C) Individual
1445 PETHs around the left goal, for place cells with a field encroaching on that goal, with a line
1446 per cell. Repeated recordings of the same cells are shown on the left and right; cells are
1447 ordered either as a function of the time of peak firing during the delay period during “Day 1”
1448 (top) or “Day 2” (bottom). Note that applying the same order to the same cells recorded
1449 during a different day (left vs right) strongly disrupts the apparent order of firing. Data for the
1450 right goal are not shown but equivalent. The color scale is as for previously shown rate
1451 maps, with red indicating a maximum normalized firing of 1 and blue indicating no firing. (D)
1452 Similarly to C, individual PETHs for out-of-field firing at the left goal. The same phenomenon
1453 is observed, namely, the apparent order of peak firing during the goal delay for a given day is
1454 not reproduced on a different recording day.

1455 **Figure 7** – Insensitivity of the population of hippocampal cells to goal value. (A) Place fields’
1456 COM distribution in all conditions; top, distribution of all place fields recorded in a 1vs0
1457 sequence (from $n = 88$ place cells); bottom, distribution of all place fields recorded in a 1-3
1458 sequence (from $n = 74$ place cells); place fields were not found to over-represent the high-
1459 value goal. (B) For illustration, cumulated (averaged) z-scored speed-filtered rate maps in all
1460 conditions (top, 1-0 sequence, $n = 88$; bottom, 1-3 sequence, $n = 74$); note how similar the
1461 pattern of firing appears across different value conditions. (C) Firing rate for all place cells
1462 with a field on a given goal zone, grouped by goal value (high or low), in the 1vs0 or 1vs3
1463 conditions, for all speeds. No difference of firing was found between the high- and low-value
1464 goals. (D) For illustration, overdispersion of the population of place cells in each condition.
1465 The numbers of passes through a place field used to build the distribution are indicated for
1466 each condition; overdispersion values are very similar for all conditions. (E) Out-of-field firing
1467 rate of all place cells without a field on a given zone, as in D, only for low (<15 cm/s) speeds.
1468 No difference was found between the two goals. (F) Normalized PETH (constructed as
1469 before) of place cells with no fields at either of the goal zones, for the low- (left) or high-

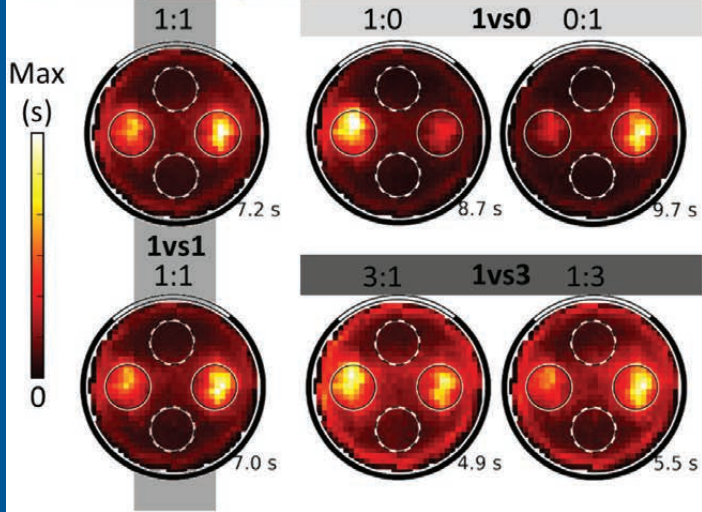
1470 (right) value goals, in the 1vs0 (top) or 1vs3 (bottom) condition. Note the reproducibility of the
1471 previously observed increase of firing during the goal period. The only difference found was
1472 between the high and low-value profiles in the 1vs0 condition.

1473 **Figure 8** – Theta power and frequency at the goal. (A) Individual example of power spectral
1474 density estimate in the theta band for 12 seconds of task behavior. Note the decrease in
1475 theta power during the goal period and the increase following reward consumption. (B)
1476 Average frequency over all 1vs1 sessions in the theta band before (-4:-2) and during (-2:0)
1477 the goal period. Note the decrease in frequency when waiting at the goal, as well as the
1478 decrease in power. (C) Top, average Z-scored power in the theta band for each 1vs1 session
1479 around the goal period (left and right goals were combined as none of the parameters of
1480 interest were different between them). White horizontal lines indicate boundaries between
1481 different rats. Middle, averaged z-scored power in the theta band, over all 1vs1 sessions.
1482 Note the decrease in theta power upon entry in the goal zone. Bottom, averaged speed at
1483 the goal for these sessions, accumulating left and right trials. Note the striking similarities
1484 between theta power and speed. (D) Z-scored theta power for each of 1vs0 sessions, either
1485 for the high-value goal (1 pellet, top) or low-value goal (0 pellet, middle). The bottom part
1486 shows the averaged Z-scored theta power, together with the average speed for the low-value
1487 goal. Note how theta power appears different between the two value conditions. (E) Z-scored
1488 theta power at the goal as for D but in 1vs3 sessions, for the high-value goal (3 pellets, top)
1489 or the low-value goal (1 pellet, middle). Averaged z-scored power and speed for the high-
1490 value goal are shown below. Note the similarity of theta power between the two value
1491 conditions.

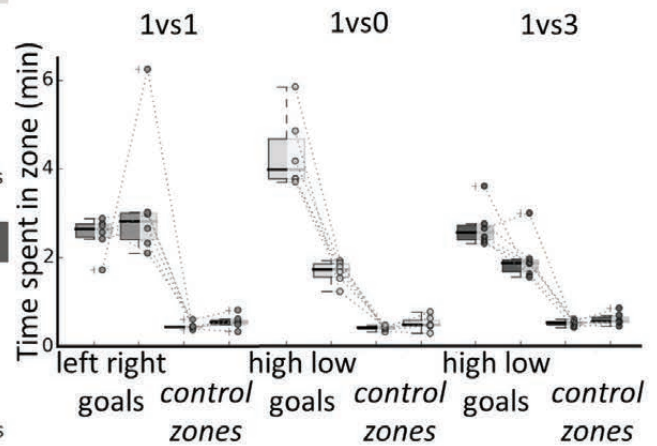
1492



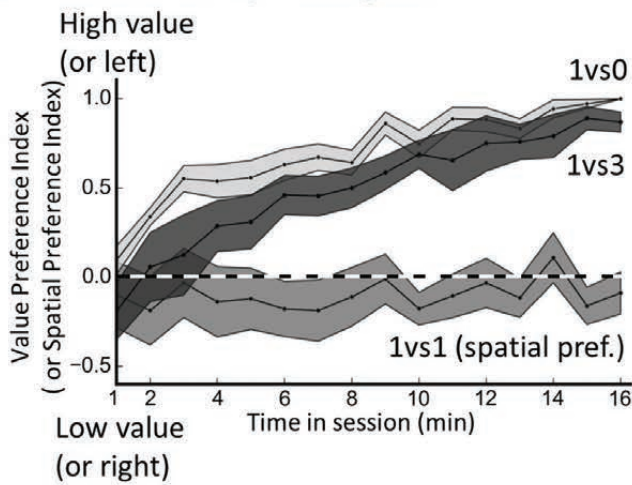
A Average occupancy



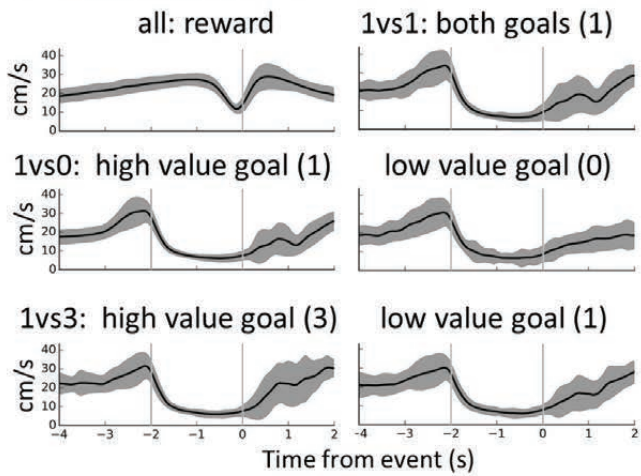
B Preference for goal zones

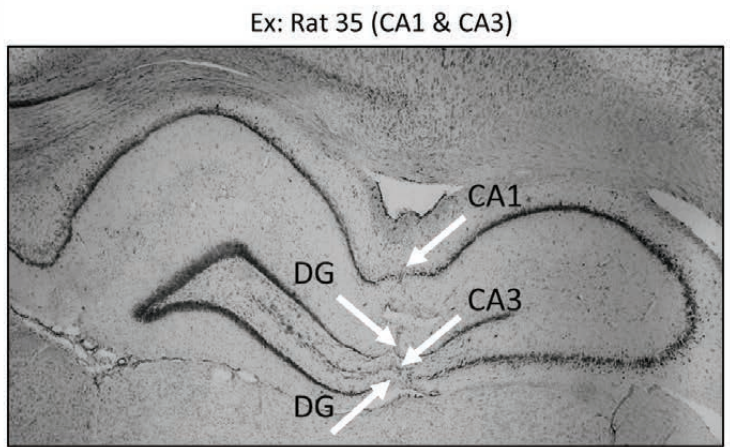
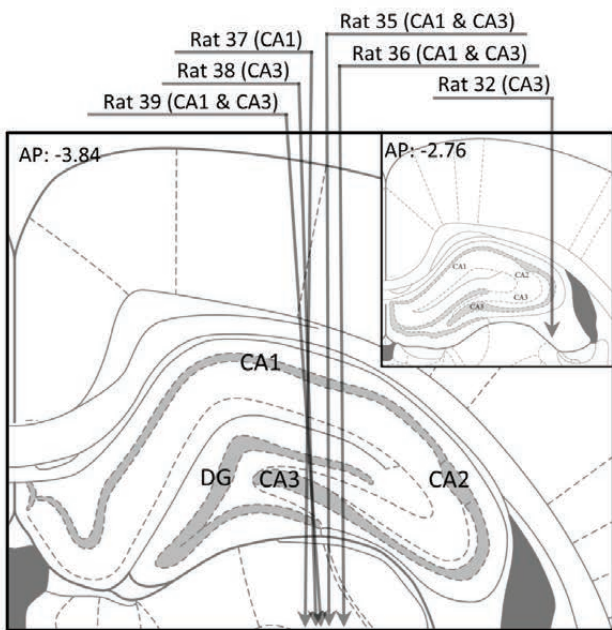


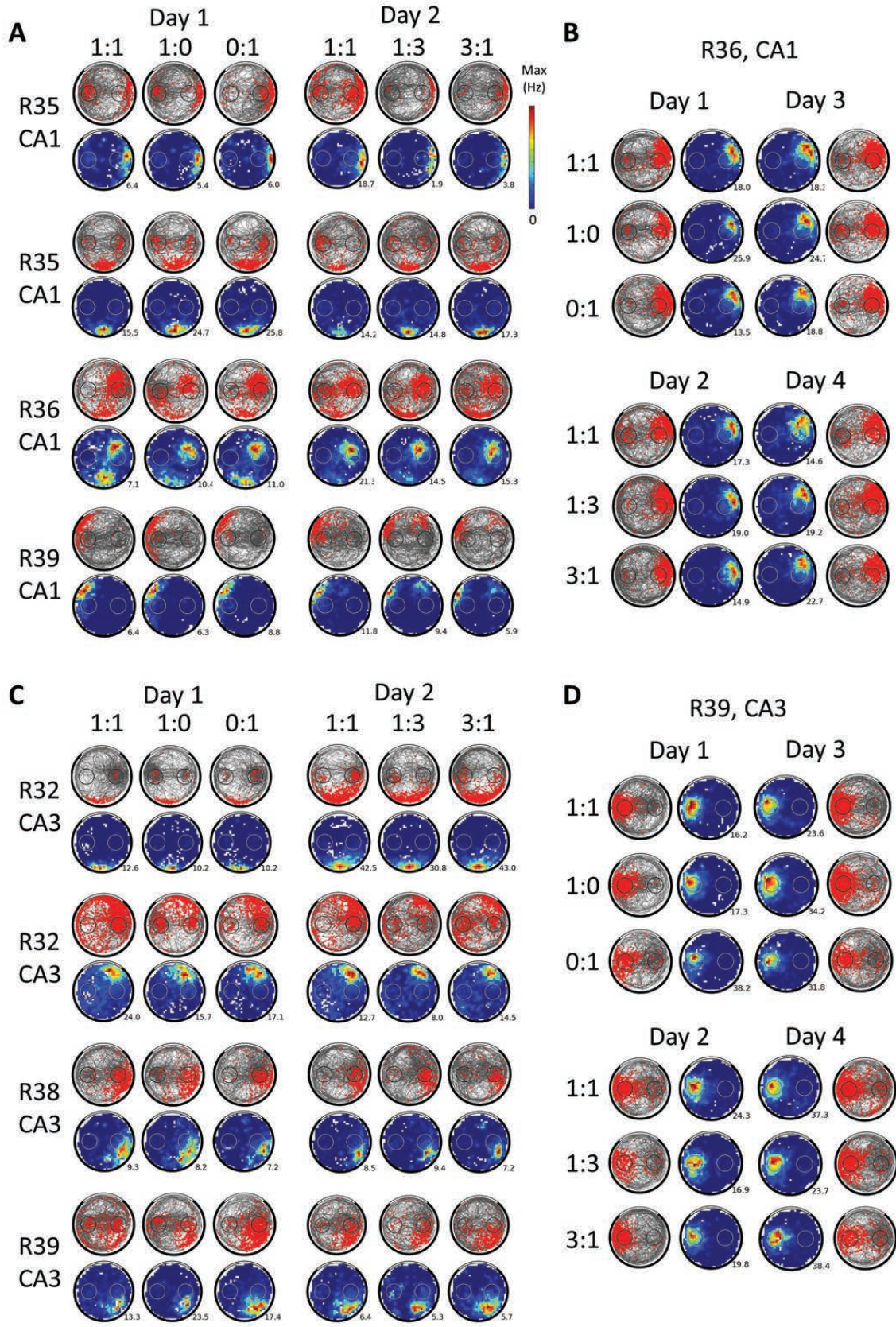
C Preference for high value goals

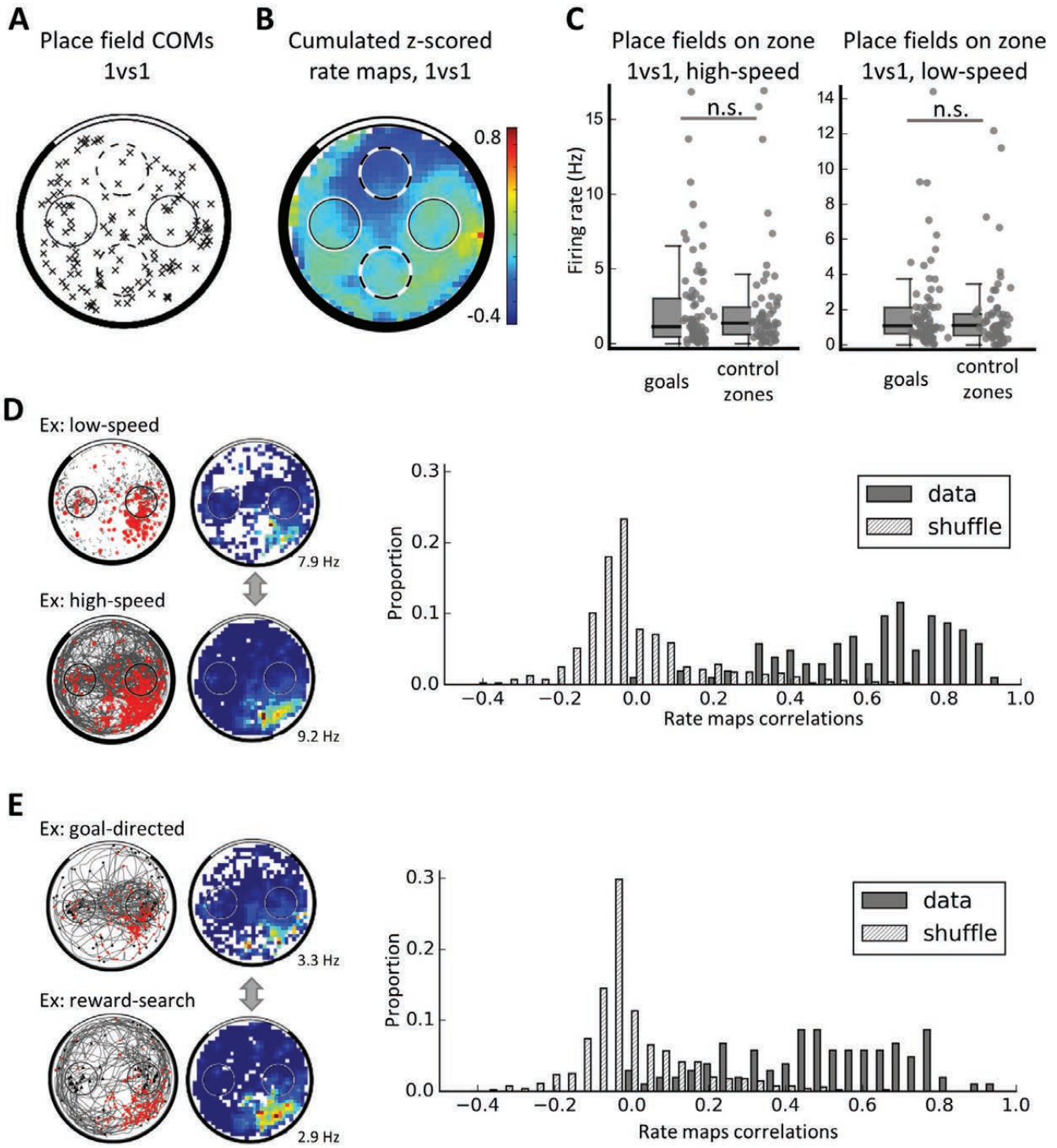


D Speed around events

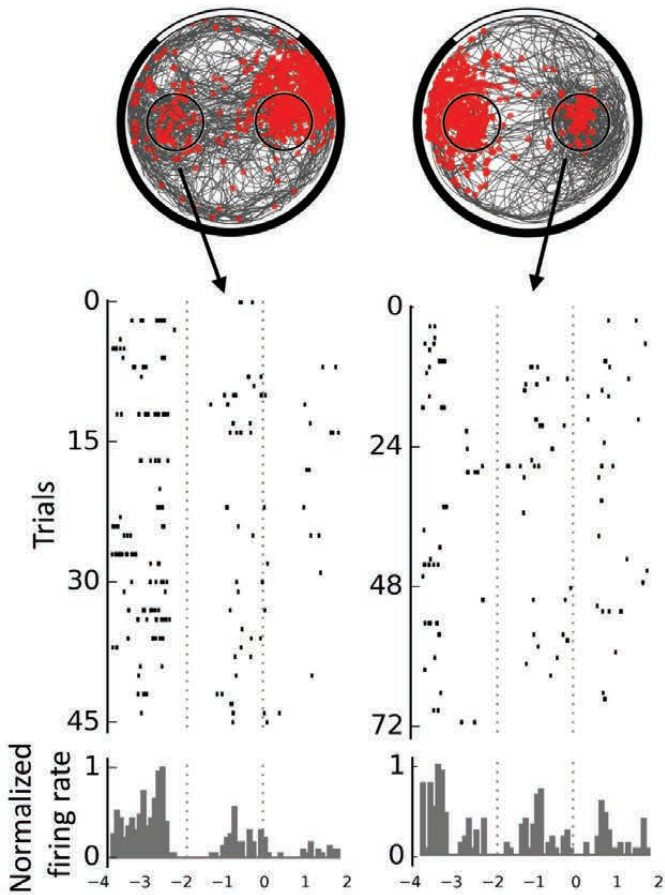




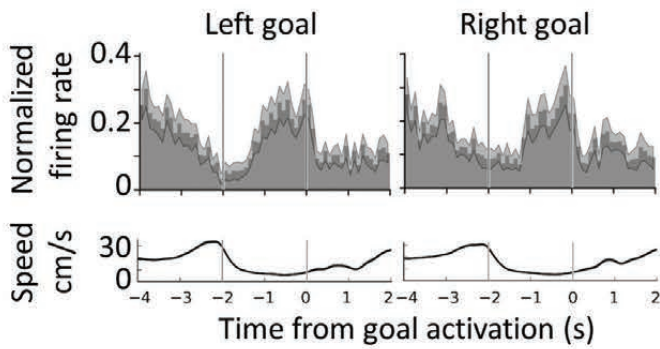




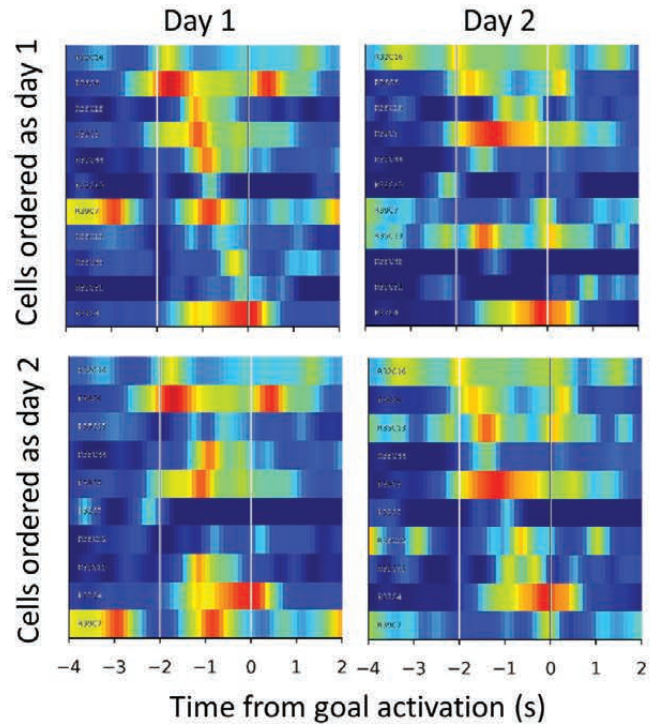
A Example cells in 1vs1



B All cells with no field at goals



C Cells with place field on goal (left goal)



D Out-of-field firing (left goal)

